Electrocomponent Science and Technology
1975, Vol. 2, pp. 75–107

ELECTRICAL BEHAVIOUR OF LANGMUIR FILMS A REVIEW: PART II

V. K. AGARWAL†

International Centre for Theoretical Physics, Trieste, Italy

(Received July 1, 1974; in final form August 22, 1974)

The electrical behaviour of thin films obtained by a variety of processes, e.g. thermal evaporation in vacuum, has been extensively studied. The study of organic mono- and multilayer films obtained by the Blodgett–Langmuir technique (commonly referred to as Langmuir films), however, has gained considerable momentum only during the past decades. Unlike evaporated films, the stiking features of these organic films are their controllable thicknesses down to one monolayer (~25 Å) and the possibility of obtaining them free from holes and conducting imperfections. The aim of this paper is to describe the film deposition techniques, some of the properties of the films so obtained and to review their electrical behaviour. It is also intended to make this review a comprehensive and up-to-date source of information for those who are either already engaged in this field or are planning to adopt Langmuir films for future investigations.

In this survey, emphasis is put on the possible problems worth further study to get more insight into the basic properties of these films. Further, since the latter possess some interesting electrical properties, this paper may prove useful in the assessment of our depth of knowledge about them and in reducing the existing gap between basic research and technological applications. Their potential usefulness in developing devices is therefore also discussed.

The survey has been divided into two parts. Part I‡ was concerned with deposition techniques, the physical properties of Langmuir films and certain electrical properties, namely dielectric behaviour and electrical conduction phenomena. This second part is concerned with electrical breakdown behaviour, voltage induced changes in electrical behaviour (forming) and ionic transport phenomena in the films and finishes, with suggestions as to future trends in work with such films together with a summary of possible applications.

To assist the reader, the two parts have been numbered consecutively with regard to sections of the text, figures and references. "Appropriate" references already cited in Part I are given again at the end of this part.

†Present address: Research Institute of Electronics, Shizuoka University, Hamamatsu-432, Japan.

‡Part I was published in *Electrocomponent Sci. and Technology*, 2, (1975).

INTRODUCTION

Films formed as mono-layers on water surfaces are of considerable interest both with regard to their theoretical behaviour and to the possible practical uses to which such films may be put when the mono-layers are transferred on to a solid substrate.[5,6] This present review is concerned with the preparation and properties of such films. It is being published in two parts, the first part having appeared in the previous issue of this journal. (V. K. Agarwal, *Electrocomponent Science and Technology*, 2, pp. 1–31, 1975.)

To assist the reader, the numbering of the two parts, both with regard to sections, figures and references has been made consecutive.

6 ELECTRICAL BREAKDOWN BEHAVIOUR

The problem of dielectric breakdown in solids has been the subject of numerous investigations. Nevertheless, the basic mechanism of dielectric breakdown has yet to be understood in all details. One of the crucial points in the breakdown process is to establish whether the breakdown results from a strictly local event or due to impact ionization. Thickness dependent studies have, however, implied that a mechanism of the latter type, presumably avalanche multiplication of charge carriers, is the prime agent of breakdown initiation. But this concept could not gain universal acceptance because some experimenters[99,100] attributed breakdown to thermal effects, i.e. the current density, even without avalanche multiplication, generated more heat in the dielectric than the dielectric itself had dissipated. Thus, the whole breakdown phenomenon seems to be based on two principal theories, *viz.*, the electron avalanche mechanism and thermal effects. Only the former, which interprets the breakdown behaviour of Langmuir films, will be discussed here. For details of these theories (both electronic and thermal) as well as the experimental data on other types of film systems reference should be made to a recent bibliographical survey of the subject[1].

On the basis of the nature of the initiating step, and of the continuation process of breakdown in thin insulating films, Klein[101] has characterized the breakdown events into three categories: a) *thermal*; b) *electronic*; and c) *electronic, modified thermal*. In the case of thermal events, the Joule heat causes a significant temperature rise resulting in an exponential rise in the electrical conductivity of the specimen. Instability arises in the field range above 10^5 V cm^{-1} when the temperature rise may be of the order of a few tens to a few hundred °C. Such events have been observed in the range 10^3–10^7 V cm^{-1} and may occur beyond this range. Electronic events occur at low fields (1–10^4 V cm^{-1}) and the temperature rise is unnoticeable, in contrast to thermal events. Such events are initiated by an electronic process such as impact ionization, double injection or the like. They have been found to occur in semi-insulating films but not in insulators. Electronic modified thermal events, have been found in a wide variety of insulating films. These events are necessarily initiated by an electronic process such as avalanching at fields typically larger than 10^4 V cm^{-1}, whose range extending from 10^5 V cm^{-1} to 10^7 V cm^{-1}. In contrast to the pure electronic event, the temperature rise may be sufficient to cause local instability by a thermal process, and current runaway occurs due either to the temperature rise or to field distortion. The electrostatic energy discharges at the instability point, leading to irreversible changes by

melting and evaporation. The electronic breakdown involves only a small volume of the specimen, in contrast to thermal instability which involves the whole uniform specimen.

To ascertain which of the breakdown events is taking place in thin films, one must know the basic underlying mechanism. The breakdown in films is particularly sensitive to specimen thickness, the nature of electrodes, the ambient medium, temperature and the type of voltages. Nevertheless, thickness dependent studies of breakdown phenomena carried out in the past few decades have led to a better understanding of the complicated breakdown mechanism. Most of the experimental data can be satisfactorily interpreted in terms of the breakdown theories assuming electron avalanche as the basic mechanism.

6.1 *Electronic Breakdown Theories*

In fact, the earliest concept of electron avalanches produced by impact ionization was predicted by von Hippel[102] and Fröhlich[103], at almost the same time in the thirties, to explain the intrinsic nature of breakdown in insulators. However, their theories failed to explain the observed data in thin films. In the subsequent development of the theories, many refinements and new suggestions were incorporated by different workers but none of them could be widely acceptable. This was so until 1964, when Forlani and Minnaja[104] made a successful breakthrough and proposed a theory of electrical breakdown in thin dielectric films. This theory could explain a wide range of existing data on thickness dependent breakdown studies and also explains the data on Langmuir films. As earlier theories have already been reviewed well (for such literature, reference is made to the bibliographical survey[1]), we shall limit our description to the recent developments in the breakdown theories made after 1964.

6.1.1 Forlani–Minnaja (F–M) Theory A fact not considered in the earlier proposed models was the origin of the charge carriers in an insulator; F–M in their theory assumed that these are injected from the cathode into the insulator by field emission and are then multiplied by impact ionization. Thus, considering the consequence of avalanche multiplication of Fowler–Nordheim emission[70], the injected current density J_{cath} can be written

$$J_{\text{cath}} = J_0 \exp\left[-\frac{4(2m)^{1/2}\phi_{\text{eff.}}}{3\hbar eF}\right], \qquad (6.1)$$

where

$$J_0 = \frac{e}{16\pi^2\hbar}\frac{(eF)^2}{\phi_{\text{eff.}}},$$

and ϕ_{eff} is the effective height of the potential barrier at the cathode-dielectric interface. Other notations have the usual meaning. The validity of Eq. (6.1) has been discussed[105] at least in the range of applied fields for which breakdown is expected. Neglecting the effect of lattice vibrations in the dielectrics in slowing down the electrons in a strong field, the number of ionizations per unit length (α) is approximately (*cf.* 69, *p.* 224)

$$\alpha = eF/I \qquad (6.2)$$

where I is the difference between the mean energy of an electron when it is able to ionize and the mean energy of electrons emerging from an ionization event. Further, considering a film thickness much lower than the recombination length, the current arriving at the anode as a result of the collision-ionization multiplication will be given by

$$J_{\text{an}} = J_0 \exp\left[-\frac{4(2m)^{1/2}\phi_{\text{eff.}}}{3\hbar eF} + \frac{eFd}{I}\right]. \qquad (6.3)$$

If it is assumed that the threshold current density above which melting or evaporation of the dielectric material occurs is of the same order as J_0, the following expression for the critical field strength is obtained:

$$F_B \simeq \left[\frac{4(2m)^{1/2}\phi_{\text{eff.}}^{3/2} I}{3\hbar e^2}\right]\left(\frac{1}{d}\right)^{1/2}. \qquad (6.4)$$

This relation evidently shows the dependence of the breakdown field on specimen thickness and has been shown to explain the experimental data for various inorganic dielectrics by Budenstein and coworkers[106–108] and for Langmuir films by Agarwal and Srivastava[109,110]. It has been discussed further by F–M that if the electron injection takes place at the negative electrode and the effective height of the potential barrier is very low, the thickness dependence of F_B is expressed as $F_B \propto d^{-1/4}$. They have thus concluded that the real thickness dependence of F_B lies between these two idealized situations.

At a later stage, F–M[111] have discussed another situation, in which the electron injection is governed by a Schottky mechanism rather than by the tunnel effect. This is expected when the applied field is very large because of the predominant role of the electron image force on the shape of the potential barrier.

Therefore, Eq. (6.1) should be replaced by an equation similar to (5.3)† in Section 5, giving the injected current density of the cathode. Following the same arguments adopted in their earlier approach[104], and by means of proper evaluation of order of magnitudes, F–M obtained the following expression for F_B:

$$F_B \simeq \frac{\phi_{\text{eff.}}}{kT} \cdot \frac{I}{e} \cdot \frac{1}{d} \qquad (6.5)$$

This equation shows the independent nature of the breakdown voltage with respect to dielectric thickness. It is valid even if the voltage drops in a non-linear way through the dielectric layer. This equation has been shown to interpret thickness-dependent data on Langmuir films in the lower thickness range[90]

It must be pointed out that Eq. (6.4) does not contain any temperature term, because the basic conduction mechanism is taken to be the tunnel effect. However, the dependence of the type $F_B \propto d^{-1/4}$, based on the electron-phonon interaction, can be shown to depend upon temperature. An increase of dielectric strength with increasing temperature would be expected, consistently with other theories based on electron-phonon scattering[102,103,112]. A reverse dependence is obtained if electron-electron scattering is properly taken into account[113].

6.1.2 O'Dwyer's Theory In spite of the fact that the F–M theory[111] is based on many simplifying assumptions, the important omission is that of space charges which arise because the positive charges left behind by the ionizing electrons were assumed to be immobile relative to the latter. O'Dwyer[114] proposed a simple theory assuming that the mobility of conduction electrons is much greater than the mobility of the holes. In considering the space charge effects, Poisson's equation is added to the current continuity, and to the heat transport equation when necessary. It was further assumed that collision ionizations are achieved only by those electrons which are accelerated from a low energy to the ionizing energy without suffering any collision with the lattice during that period. With these assumptions, the functional dependence of field strength with the dielectric thickness could be expressed in terms of certain dimensionless parameters, although no explicit form was given for the function itself.

† $J = AT^2 \exp\left(\frac{\phi_0}{kT}\right) \exp\left(\frac{\beta_S F^{1/2}}{kT}\right)$ (5.3)

The fact is, however, that the data on thickness dependence of the breakdown strength could not be explained by fitting it in terms of the dimensionless parameters, i.e. dimensionless mean field strength and dimensionless dielectric thickness. When F–M[111] pointed out the above difficulty, O'Dwyer[69,115] made further progress and proposed a more realistic model. Now he assumed that highly mobile electrons injected into the insulator at the cathode by field or thermionic emission produce avalanching, and that the current is totally electronic. Again he obtained the set of equations and solved them for the steady state. The highest field, below which the instability and current runaway might arise, was taken to be the dc breakdown field.

Whereas O'Dwyer's modified theory could explain the data of various experimental investigations on alkali halides, it did not prove to be so successful for thin films. For example, it failed to interpret the destruction of the film at higher current densities and lower fields, because the model is based on the current instability criterion rather than the condition for destruction. It has been pointed out by Klein[116] that the earlier theories as well as the above theory assume uniform charge injection and avalanching in the whole specimen, whereas in practice the situation is different. He has shown quantitatively that the continuum theories, such as O'Dwyer's, do not explain the breakdown event adequately if it is a consequence of localized avalanches which are spaced widely from each other.

6.1.3 Klein's Localized Electronic Breakdown Theory The concept of localized breakdown was given in earlier theories of Fröhlich[103] and Seitz[112], but these theories were based on single electron avalanche and do not include the effect of space charge, and the occurrence of instability prior to destruction. Following the suggestion by Watson *et al.*[117] that a rapid sucession of avalanches may produce the breakdown, Klein[116] has developed a model to show how a succession of avalanches can produce breakdown in thin films. This model, in fact, explains the dependence of breakdown phenomena on almost all the parameters, and is supported by a wide variety of experimental data. However, only essential points will be discussed here, which are relevant in the context of the present paper to explain the data on Langmuir films.

According to the proposed statistical model assuming localized electronic breakdown, the breakdown is initiated by electron injection into the conduction band of the insulator, and develops in a

sequence of stages. The injected electron (by field emission or thermionic emission) at the cathode produces an avalanche of free electrons by impact ionization, and the positive charges are left behind in the insulator. The latter, being nearly immobile, drift slowly to the cathode and form a positive charge cluster which results in the enhancement of the cathode field. The local electron injection rate is thus increased and a finite probability reached for an electron to be injected during the transit of the charge cluster through the insulator. Consequently, there is further avalanching which in turn accelerates the breakdown process in insulators. Since the local cathode field during the transit of the charge cluster increases with the avalanche length, the formation of large avalanches also depends upon the film thickness, in addition to the many other parameters involved.

In the present model, the ionization coefficient α has been assumed to obey the relation $\alpha = F/V_i$ which was proposed by Shockley[118] for "high fields" applicable to semiconductors; F is the applied field and V_i is the ionization voltage. This was found suitable in view of the fact that the observed breakdown fields extended over a wide range in most insulators. However, it has been shown that the proposed theory also interprets the breakdown events at the "low fields", obeying the relation proposed in O'Dwyer's model[119] for α. The mean avalanche length a_v has been shown to depend upon α by the following relation:

$$a_v = \frac{Ki}{\alpha} = \frac{KiV_i}{F}, \tag{6.6}$$

where $K > 1$ is a factor taking account of the average increase of the mean free paths for ionization towards the anode, and i is the number of collisions of the injected electron while travelling through the insulator. It has been shown that the effective field acting on the electrons in the film is so low beyond a_v that no more impact ionization occurs when a_v is not much smaller than the insulator thickness d.

Now, if the film is too thin ($d < a_v$), avalanche cannot develop and the probability of breakdown becomes very small. Therefore, for breakdown to occur even at relatively low rates, it is necessary to raise the applied field to an extent that $a_v \leqslant d$ or from Eq. (6.6)

$$F \geqslant \frac{KiV_i}{d}. \tag{6.7}$$

Evidently, this shows that the breakdown field (at which breakdown begins to occur) in very thin insulators is inversely proportional to the thickness d. Further, it has been shown for $d > a_v$, that the rate of decrease in the breakdown field with increasing d becomes smaller for all values of mean time to instability. The observed experimental data on Langmuir films (discussed later in this section) support the predictions of this theory.

As regards temperature effects on the breakdown field, it has been shown that these vary with the nature of the injection current process, the hopping mobility and the ionization coefficient values. To predict the temperature effects on electronic breakdown events, one must determine how the above parameters change Consequently, some of the temperature effects promote, and others oppose the development of breakdown. Experimentally both types of behaviour of the breakdown field (increasing and decreasing with temperature) have been observed in various thin film insulators.

This theory of localized electronic breakdown in insulating films has been shown to interpret the observed data of various types of film systems over a wide range, including almost all the parameters, such as temperature, thickness, electrode material, space charge, etc., which are known to affect the breakdown phenomena. In addition, one of the most successful features of this model is that it also explains the completion of the breakdown event, including the destruction of the insulating film. It has been discussed that the breakdown follows in a sequence of stages, i.e. in the initiating stage, harmless avalanches occur in the whole specimen and the temperature rises during the avalanching of electrons. Consequently, a significant enhancement of the electrical conductivity takes place, which causes voltage collapse through a current runaway. Impact ionization may stop during the latter stage, but the breakdown events continue until destruction occurs because of the thermally unstable state, due to temperature rise at the site. Thus, a complete breakdown event mainly comprises the initiation of breakdown, instability due to heating, and finally the destruction of the capacitor with voltage collapse. In the author's opinion, Klein's proposed model is the most successful approach among those discussed by various workers. Nevertheless, it does not take into account explicitly the presence of defects in the insulating films, and future work might improve the theory further.

6.2 *Experimental Studies on Langmuir Films*

Langmuir films of fatty acid salts are known to have high breakdown strength $\simeq 10^6$ V cm^{-1} for a long

time. The earliest studies of the breakdown of the films under high dc voltages were carried out by Porter and Wyman[46]. The experimental arrangement employed for such measurements was very simple, consisting of a galvanometer to read the current. Using a Hg drop as the upper electrode, no current was detected until the voltage applied across the specimen reached a certain critical value in the case of 30-layer thick films, whereas with thinner films, appreciable currents were present almost from the start. The breakdown per layer was found to rise sharply at a thickness of about 20 layers, and its order of magnitude was $\simeq 10^6$ V cm^{-1}. Very high specific resistance $\simeq 10^{13}$ Ω, below the breakdown voltage was found. Later the Hg droplet was replaced by a drop of tap water, and the device behaved almost the same way as with Hg. However, there was one striking difference, in that the critical voltage at which there was a sudden rise of current was independent (nearly) of film thickness. It was higher for thin films, and lower for thick films, than for corresponding cases using mercury. No striking difference was observed in the breakdown voltage of X and Y films, and some difference in $I-V$ characteristics is attributed simply to electrical asymmetry in the film, probably associated with the initial layer. Further, the film was disrupted permanently when the breakdown voltage was exceeded with mercury drops. On the other hand, with water drops there was no change in the nature of the $I-V$ curves even after the film had been subjected to a voltage beyond the breakdown point. The difference has been ascribed to the different affinities of the two liquids for the surface, and presumably the water molecules were able to penetrate the film.

Similar attempts were made by Race and Reynolds[43] in the early period, and data was collected on films of cadmium arachidate obtained from solutions of varying pH values in the range 5.1 to 6.62. As is known, the proportion of conversion to soap depends upon the pH of the solution, the highest dielectric strength was found only at higher pH values, which correspond to a higher proportion of converted soap. Experiments on skeletonized films showed lowering of dielectric strength, as expected. Further measurements on dielectric strength as a function of frequency showed a wide scatter in the observed data, and thus no conclusion could be drawn. However, at 1000 Hz, the highest values were obtained. Race and Reynolds were unable to prevent the inclusion of dust particles in the multilayer films, and therefore the data, in general, were disappointing. Nevertheless, they succeeded in depositing 201-layer thick films that could withstand from 150 to 190 V, corresponding to a dielectric strength of 2×10^{-6} V cm^{-1}. Because of the difficulty in obtaining large areas of the films free from cracks, holes or dust particles, the possibility of using such films as practical capacitor dielectrics was ruled out in their work.

Evidently, these earlier measurements do not predict anything about the breakdown mechanism, and no efforts were made by these workers to interpret their data in terms of any known theory at that time. Other attempts also yielded only the orders of magnitude of dielectric strength of Langmuir films. For instance, Thiessen *et al.*[120] were able to apply electric fields up to 5×10^6 V cm^{-1} on barium and calcium stearate film capacitors in the thickness range 100 Å–1000 Å. Similarly, Holt[29], while considering the use of Langmuir films as thin film dielectrics, reported the dielectric strength to be $\simeq 10^6$ V cm^{-1} for varying thickness range of barium stearate films. It was not until the last few years when Agarwal and Srivastava[109,110,121–123] reported detailed and systematic investigations on thickness-dependent behaviour of breakdown strength (dc and ac) of various fatty acid soap films. Such studies were undertaken to illustrate the underlying breakdown mechanism, as well as to obtain information about the breakdown strength over a wide range of film thicknesses, which is of fundamental importance for the development of devices. Similar measurements of temperature dependent behaviour[124,125] were also undertaken in the same school, and some preliminary measurements[123] on the ac breakdown strength of barium stearate films were carried out. In the following section all experimental investigations have been reviewed.

6.2.1 Thickness Dependent Studies In the studies Agarwal and Srivastava[109,110,121,122] (dc) a capacitor geometry of Al–film–Al has been used, and the thickness range covered is 1–80 layers, corresponding to 25 Å–2000 Å. In their earliest investigations on barium stearate films[109] Hg drops were used as the upper electrode. Three principal breakdown voltage thresholds, *viz.* onset breakdown, destructive breakdown and maximum breakdown voltages have been encountered. These have been distinguished by the initial abrupt rise in the current, by the commencement of "visible" destruction in the film and by the destruction of the film capacitor over large areas, respectively, when the applied dc electrical field was increased linearly across the capacitor. For the sake of simplicity, we shall describe here the data in two

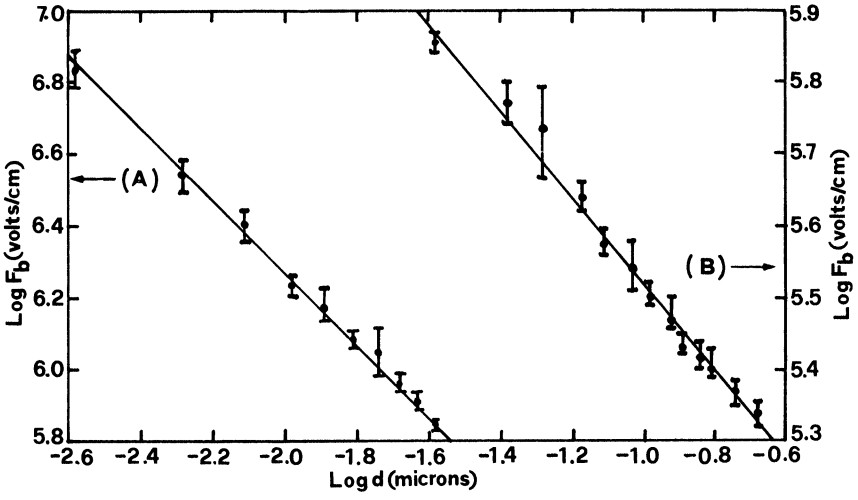

FIGURE 22 Plot of log F_b vs. log d for Al-barium stearate-Hg devices. Curves (A) and (B) correspond to the thickness range 25–250 Å (1–10 layers) and 250–2000 Å (10–80 layers), respectively. The bars represent the scatter in the experimental data at a particular thickness and the dots correspond to the mean values of several observations made on different samples of the same thickness. [After Agarwal and Srivastava[109].]

parts, one consisting of onset breakdown voltages when there is no destruction of the film, and the other consisting of both the latter events of the destructive type.

6.2.1.1 *Onset breakdown voltage* Measurements of dc onset breakdown voltage are carried out[109,110,121] on mono- and multilayer Langmuir films of barium palmitate, margarate, stearate and behenate. Figure 22 shows a log-log plot of breakdown field F_b versus film thickness d on barium stearate films. The dielectric strength is always found to be a power-dependent function of the film thickness d, i.e. $F_B \propto d - \alpha$ with α varying in the different thickness ranges. The curve (A) in Figure 22 is a plot corresponding to 1–10 layers, and the curve (B) corresponds to the higher thickness range of 10–80 layers. Evidently $\alpha = 1.01$ in the lower thickness range (25–250 Å) and $\alpha = 0.59$ (approximately) in the higher range (250–2000 Å). Similar values of $\alpha = 1.08$, 1.08 and 1.02 (for 1–10 layers) and $\alpha = 0.52$, 0.52 and 0.53 (for 10–80 layers) were obtained for barium palmitate, margarate and behenate films, respectively. Agarwal and Srivastava[109,110] interpreted their results in the higher thickness range in terms of F–M theory[104] of breakdown for small thicknesses, which predicted α to be 0.5 for the high energy gap dielectrics, and for low electron affinity (Eq. (6.4)). However, for the results in the lower thickness range, it was proposed that these may be explained in terms of the increased boundary scattering[109,121].

In a recent communication, Srivastava[90] has explained the above results in the lower thickness range in terms of the F–M theory[111], which considers a transition from tunnelling to the Schottky effect because of the predominant role of the electron image force. Evidently, Eq. (6.5) thus explains these results, showing the independent nature of the breakdown voltage with respect to film thickness. Based on this interpretation, Srivastava[90] has proposed that the breakdown data in the lower thickness range of Langmuir films constitute evidence of Schottky dominated dielectric breakdown in these films. It is also pointed out that the breakdown field for 10 monolayers (thickness ≃250 Å) may be regarded as near the "transition field" of these films, which is not possible to calculate theoretically mainly because of the unknown band structure parameters of the insulating films. The author[126], however, has discussed recently that it is premature to agree fully with the evidence of Schottky dominated mechanism in Langmuir films[90]. This is because most of the data on the conduction mechanism in these films have shown that electron tunnelling is the operative conduction mechanism in the lower thickness range. Further, Eq. (6.5) also shows an explicit dependence of the breakdown field upon the temperature. Unfortunately, no experimental work seems to have been reported showing temperature effects in the

breakdown field in the lower thickness range, which would support the contention of Schottky-dominated breakdown in these films. Even the work by Agarwal and Srivastava[124] on barium stearate films (thickness ≃515 Å) in the temperature range −40°C to 40°C neither corresponds to the thickness range under consideration nor conforms to the F–M theory[111] based on electron-phonon interactions.

On the other hand, it has been shown that Klein's statistical model[126] is much more realistic for the interpretation of the present thickness dependent data in the lower range. Obviously, Eq. (6.7) explains the observed thickness independent nature of the breakdown field at which breakdown begins. The relevance of this theory in the present context is supported by the fact that the whole breakdown phenomena from its inception to completion has been interpreted by Klein's theory in a recent communication[127]. One of the limitations of the F–M theory is that it does not interpret the occurrence of destruction of the film due to thermal instabilities developed at high applied fields.

6.2.1.2 *Destructive breakdown* Destructive breakdown in Langmuir films consists of two events, i.e. the destructive breakdown voltage and the maximum breakdown voltage. These events have been determined in various fatty acid soaps in the thickness range corresponding to 16–80 layers[121,122]. Figure 23 shows a typical plot of current density J versus applied voltage V in the non-destructive phase for a 40-layer barium stearate film having area ≃0.5 cm^2. The point A in this curve (Figure 23) corresponds to the initial abrupt rise of current (onset breakdown voltage) and the point B corresponds to the destructive breakdown voltage V_{db} at which the "visible" destruction of the film commences. It has been reported by Agarwal and Srivastava[122] that the J–V characteristics could not be traced beyond this point B because of the fluctuations. Evidently, the two breakdown voltages are widely different from each other. When the applied voltage was increased beyond V_{db}, a large area of the film capacitor was found to be destroyed at maximum breakdown voltage V_{max}. Figure 24 shows a typical transmission microphotograph (x40) of a barium stearate film capacitor (area ≃0.4 cm^2, thickness ≃400 Å) at an applied voltage of 84 V when a series resistor (≃5K) was used in the circuitry. The destructive breakdown voltages were found to be independent of the material and thickness of the film. But the maximum breakdown voltages varied slightly with increasing film thickness. The corresponding maximum breakdown strength, F_{max}, was found to be a function of thickness d of the type $F_{max} \propto d^{-\alpha}$ with $\alpha = 0.95$, 0.95, 0.96 and 1.00 in barium palmitate, margarate, stearate and behenate, respectively. A typical plot showing the variation of maximum breakdown strength F_{max} with thickness d has been given (Figure 25). This is a log-log plot for barium stearate films in the thickness range corresponding to 16–40 layers, and gives $\alpha = 0.96$. The maximum breakdown strength thus determined was ≃10^7 V cm^{-1} in all the films.

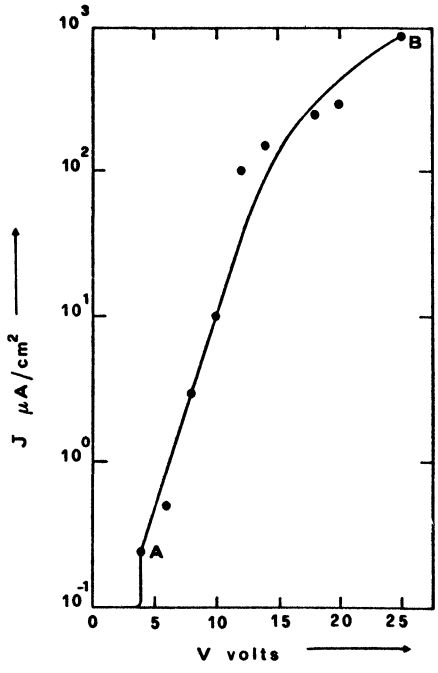

FIGURE 23 V–J characteristic in the non-destructive phase for a 40-layer barium stearate sandwich with area ≃ 0.5 cm^2 at room temperature when the series resistor (≃ 5K) between the source and device was connected. Point A represents the "onset breakdown voltage" and B the "destructive breakdown voltage" of the device. [After Agarwal and Srivastava[122].]

Such studies on a variety of evaporated dielectric films have also been made in the extensive work of Klein (reviewed in 128), and Budenstein and his coworkers[106–108]. However, they had different opinions, at certain points in their discussion of the destructive breakdown events in thin films. For example, Klein and Gafni[100] (K–G) classified these events as single hole, propagating and maximum voltage depending upon various factors such as capacitor dimensions, circuitry employed and voltage wave form applied. They stated that breakdown is

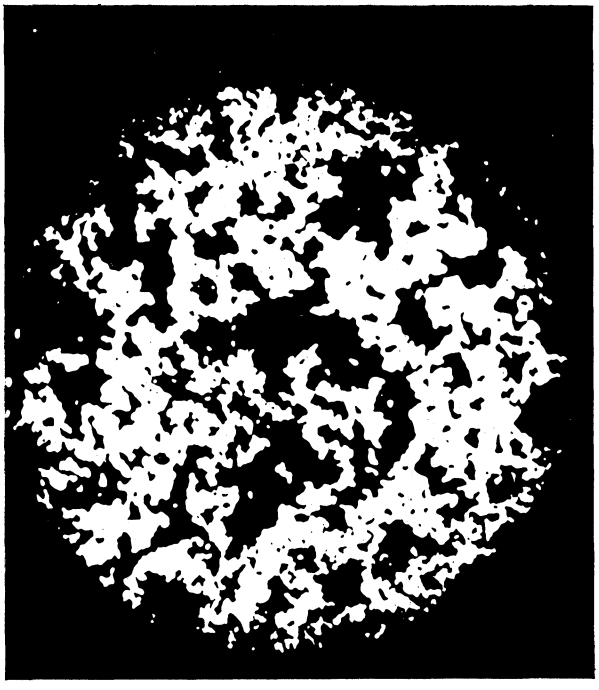

FIGURE 24 Transmission photomicrograph showing the destruction of the film capacitor (area $\simeq 0.4$ cm^2) of thickness $\simeq$400 Å at 84 V when the series resistor ($\simeq$5K) was used. [After Agarwal and Srivastava[122].] x 40.

thermal in origin in silicon monoxide. Budenstein and Hayes[106] (B–H) did not agree stating that the breakdown is not thermal and showing that the classification proposed by K–G is purely phenomenological. Another suggestion of K–G, that the maximum voltage breakdown encountered in their studies is a characteristic of the bulk, also disagreed with B–H. Based on these counter-interpretations, Agarwal and Srivastava[121,122] distinguished their "maximum breakdown voltage" from that observed by K–G, showing that it determines the "ultimate dielectric strength" of the dielectric for all "practical" purposes and is not a characteristic of the bulk. Further distinction has been made by stating that the device is of the self-healing non-shorting nature, and therefore the single hole and propagating breakdowns could not be observed under the microscope in transmission. Except for the fact that an attempt was made to establish the non-thermal nature of breakdown events in Langmuir films, based upon the above considerations and considering also the electronic nature of onset breakdown voltage, no satisfactory interpretation could be given for the studies on destructive breakdown.

However, the author[127] has tried to interpret the whole range of breakdown events in Langmuir films in terms of the recently proposed Klein's statistical model[116]. Three breakdown events of Langmuir films have been related to the respective stages of breakdown completion. Presumably, during the initial stages of voltage applications, harmless avalanches occur; with increasing field, the local instability becomes high enough at a particular site causing the "visible" destruction and, finally, a large area of the capacitor is destroyed by some sort of conducting channel, until the high-voltage, low-current stage is reached. The lack of destruction in the intermediate stage has been explained in terms of the discharge of electrostatic energy only through a small area of the capacitor. The whole breakdown is assumed to advance through a series of consecutive localized breakdowns, which is a characteristic of the weakest spots in the organic film. The first two events have been shown to be electronic in nature, and the last is a thermal event because of the temperature rise during the avalanching process leading to melting and/or evaporation of the material. Thus, the breakdown process in Langmuir films has been described as an 'electronic, modified thermal" event. The microphotograph (Figure 24) is regarded as an illustration of "propagating breakdown" like that observed by K–G[100]. Even now the thickness dependence of maximum breakdown voltage remains inexplicable because no such breakdown theory is yet available. Nevertheless, the higher values of the breakdown strength are in agreement with those of Race and Reynolds[43] who found that a 201-layer thick multilayer could withstand from 150 to 190 V.

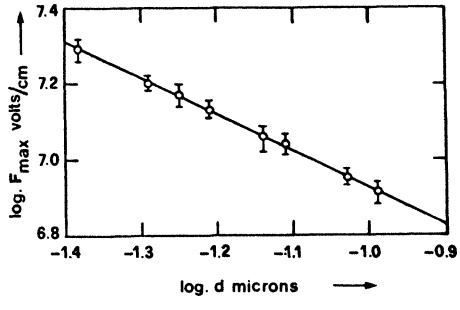

FIGURE 25 Log-log plot of maximum breakdown strength F_{max} vs. film thickness d for barium stearate films in the thickness range (400 Å–1000 Å) at room temperature. The dots and bars represent the same relationship as in Figure 22. [After Agarwal and Srivastava[122].]

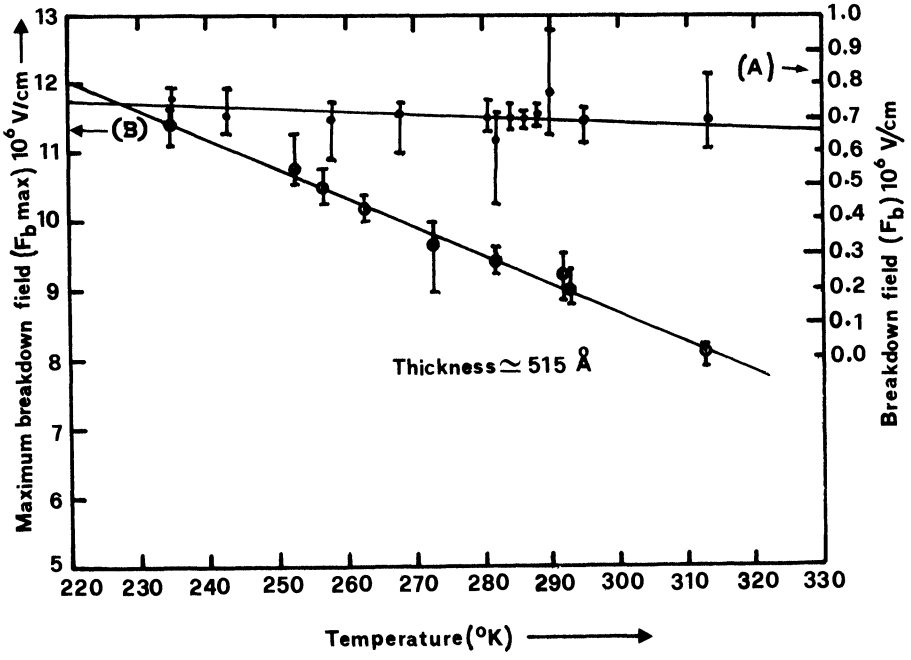

FIGURE 26 Curve (A) showing breakdown field F_b vs. temperature T for Al–20 layer barium stearate–Al sandwich in the temperature range −40 to +40°C. Curve (B) shows $F_{b\,max}$ vs. T for a similar specimen as in (A). The bars and dots indicate the same relationship as in Figure 22. [After Agarwal and Srivastava[124,125].]

6.2.2 Temperature Dependent Studies An attempt to investigate temperature dependent characteristics of Langmuir films was made by Agarwal and Srivastava[124,125] after it was realized that thickness-dependent data furnish reliable information on the breakdown mechanism. Such studies were thought desirable, particularly because the devices must operate at various temperatures. The onset breakdown strength F_b[124] and the destructive breakdown strength $F_{b\max}$[125] of barium stearate films have been studied as functions of temperature in the range −40°C to +40°C. The capacitor geometry used was Al–film–Al and the two breakdown events were distinguished on the same lines as discussed in the thickness-dependent studies. Curve (A) in Figure 26 shows the plot of temperature versus breakdown field F_b for a barium stearate film (thickness 515 Å). Evidently, F_b decreases slowly with increasing temperature, which is similar to that observed by Budenstein and co-workers[106–108] in some evaporated thin film systems. Theoretically, such behaviour is expected, provided that the electron-electron scattering is properly taken into account. However, these workers failed to interpret the results in terms of any electronic breakdown theory based on electron-phonon scattering[102,103,112] or in terms of the recent F–M theory, which shows an increase of dielectric strength by increasing the temperature (see Eq. (6.5)).

Further, these workers[125] obtained data on the temperature dependence of the destructive breakdown field $F_{b\,max}$ in barium stearate film capacitors, and found that the decrease of $F_{b\,max}$ with increasing temperature is more rapid than that of F_b. Curve (B) in Figure 26 is a typical plot of $F_{b\,max}$ with respect to the temperature of a barium stearate film (515 Å thick). These results could not be explained, however, because no theory is yet available to account for temperature effects on the destructive breakdown field. In fact, the temperature behaviour of electronic breakdown events is not yet well understood either theoretically and experimentally. The recent Klein model[116] explains the possibilities that breakdown strength can either increase or decrease with increasing temperature, depending upon the nature of electron injection which affects the mean time to instability, and consequently the breakdown strength. J–V characteristics plotted in the work of Agarwal and Srivastava[124,125] and the transmission photomicrograph of the capacitor at destructive breakdown voltage do not provide any more information than that obtained in thickness-

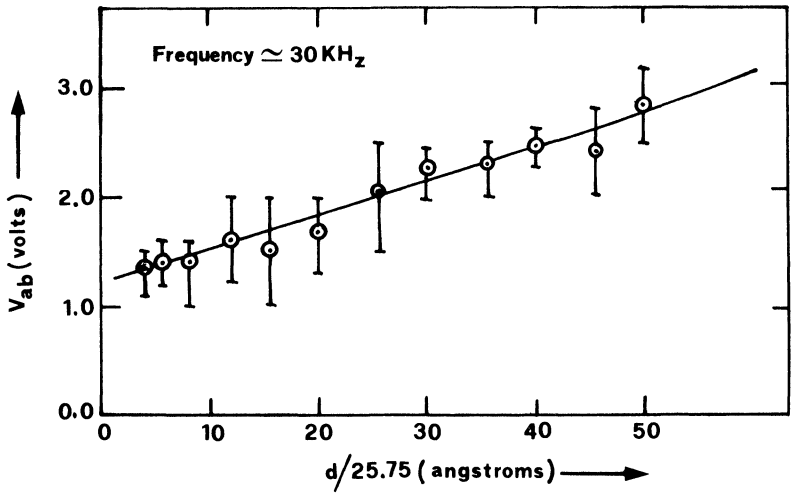

FIGURE 27 Plot of ac breakdown voltage V_{ab} vs. film thickness **d** of barium stearate at fixed frequency ≃ 30kHz in the thickness range 100 Å–1500 Å. The relationship between dots and bars is the same as in Figure 22. [After Agarwal and Srivastava[123].]

dependent studies. The breakdown voltage has, however, been found to decrease with increasing capacitor area in agreement with the observations of Budenstein *et al.*[107].

6.2.3 AC Breakdown Studies In these preliminary measurements of ac breakdown[123], the onset breakdown strength V_{ab} has been studied as a function of thickness and frequency, in the thickness range 100 Å–1500 Å, and in the frequency region 10–200 kHz. Barium stearate films were always sandwiched between two aluminium electrodes and the occurrence of breakdown was inferred from an abrupt rise in the current. Figure 27 shows the behaviour of ac onset breakdown voltage V_{ab} (peak value) with film thickness d at a fixed frequency of 30 kHz. Evidently V_{ab} increases with increasing film thickness. When the corresponding breakdown strength F_{ab} was plotted as a function of thickness d on a log-log scale, it was found that $F_{ab} \propto d^{-\alpha}$ with

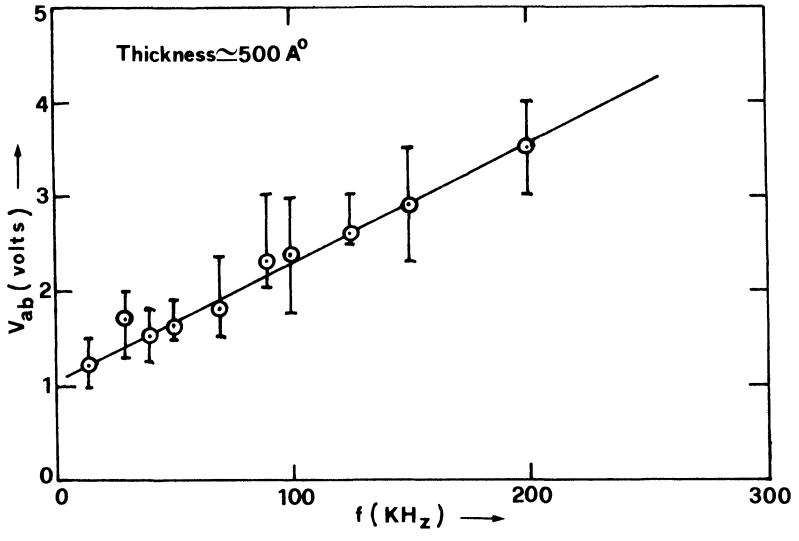

FIGURE 28 AC breakdown voltage V_{ab} vs. frequency **f** for barium stearate film of thickness 500 Å in the frequency region 10–200 kHz. The relationship between bars and dots is similar to that indicated in Figure 22. [After Agarwal and Srivastava[123].]

$\alpha = 0.68$. Incidentally, this is the same behaviour as these workers[109,110] had already obtained in their corresponding dc studies. Further, a graphical representation of V_{ab} versus frequency f for a film of thickness 500 Å (Figure 28) shows that V_{ab} increases with increasing frequency. Similar studies were carried out by Klein and Levanon[129] on SiO films and three types of ac breakdown processes were distinguished, as were found in their dc investigations[100]. A theory was also proposed by Klein and Levanon[129] which was based on the thermal nature of breakdown, and predicted a decrease of breakdown strength with increasing frequency for the high-frequency range studied. In view of the observed contradictory experimental data in Langmuir films, Agarwal and Srivastava[123] deduced that the breakdown is non-thermal in nature. Fortunately, the electronic nature of the first breakdown event has already been established by these workers through their dc investigations.

The experimental data could not be interpreted because of the lack of an ac electronic breakdown theory. It has been pointed out, however, that in spite of the high structural perfection of these films, the breakdown is, presumably, initiated as "single hole" breakdown. The scatter in the experimental data has been attributed to the inevitable voids and the inhomogeneities in the deposited film, as well as to the effects of electrode thickness which, of course, the authors tried to control in their measurements. The onset ac breakdown strength of barium stearate films, in order of increasing film thickness, was found to lie between 1.33×10^6 and 0.22×10^6 V cm^{-1}, which is lower than the corresponding dc breakdown strength ($1.75 \times 10^6 - 0.27 \times 10^6$ V cm^{-1}). This observation is supported by the observations of Race and Reynolds[43] who obtained higher values for dc breakdown strength than the ac values.

The situation regarding breakdown phenomena in Langmuir films can best be summed up by saying that it is not yet well understood. Although thickness dependent studies could be interpreted adequately in the light of existing theories, these are not enough to make sure what exactly is the underlying conduction mechanism. On the other hand, the temperature dependent data are in a primitive stage and cannot be interpreted. Many factors may be pointed out in these studies which, if taken into consideration would lead to a better understanding of the whole phenomenon. To list a few; the breakdown rate has not been investigated and the $I-V$ characteristics are recorded only up to the stage of destruction. Even the $I-V$ characteristics do not give sufficient information about the pre-breakdown conduction. The influence of the oxide layer formed between the base aluminium electrode and the film has also not been discussed.

Whereas these factors must be considered in future works, more attention must also be paid to the determination of breakdown strength as a function of the electrode material, polarity of applied voltage, ambient conditions and nature of the applied voltage wave form, etc. A few groups, e.g. Klein and co-workers, Budenstein *et al.* and Osburn's group have been actively engaged in the study of breakdown behaviour of varied types of dielectric films, and each of their papers contains new information. The reader is therefore advised to refer to their original papers describing their studies on evaporated films. The recent bibliographical survey[1] on breakdown conduction in thin films is a comprehensive and up-to-date collection of such literature.

One of the most significant contributions of Agarwal and Srivastava, is the determination of breakdown strength over a range of three decades of thickness which is very useful from the device applications point of view. The reliability of these data lies with the fact that the onset breakdown strength, which is of prime importance in device applications, has been found to fit the theories very well over the whole range for all types of Langmuir films studied. AC breakdown and temperature dependent behaviour have been studied only on barium stearate films, and hence more experimental work must be done before one can place too much reliance on these data. Presumably, the recently proposed theories must also be modified to explain the observations of the latter two types of experiments on Langmuir films. Necessarily, further development in the understanding of electrical breakdown will depend on appropriate experiments. Thought must also be given to identification of the physical mechanism, in addition to study of the dependence of breakdown strength on various parameters.

7 FORMING PROCESS AND DIFFERENTIAL NEGATIVE RESISTANCE

The application of voltage greater than a minimum, V_F, across a metal-thin film insulator-metal device may cause a radical and essential change in its electrical properties, such as a large permanent increase in the conductivity. This process is desig-

nated the "forming" process, and V_F is known as the "forming voltage". This process has been found to occur most readily in many thin film insulators with reactive anions, such as oxides (SiO_2, Ta_2O_5, Al_2O_3) and fluorides (CaF_2, MgF_2, MnF_2), and was thought to be a characteristic feature of non-stoichiometric insulators. After the sample was "formed", the device also showed a pronounced differential negative resistance (henceforth DNR) in its $I-V$ characteristics. Until a few years ago, DNR behaviour was established only for amorphous or polycrystalline insulators. Recent investigations on Langmuir films[130,131] have shown that DNR also occurs when organic monolayers sandwiched between metal electrodes are formed. Therefore the phenomena under consideration are to a large extent independent of specific properties of the insulating material. However, some distinct differences were observed in the case of organic monolayers, which will be described in the following discussion. Before we proceeed to discuss the DNR in Langmuir films, some of the characteristic features of the "forming" process will be outlined, and the models to explain the process will be discussed briefly. For greater details on the subject the reader is referred to a recent review paper[132].

7.1 *Factors Influencing Forming*

The major factors which influence the degree of forming are the applied voltage and its nature, temperature, atmospheric conditions in vacuum, insulator thickness and the electrode material. Application of a voltage pulse ($\geqslant V_F$) of a few seconds duration, or a sinusoidal voltage of amplitudes greater than V_F at room temperature "forms" the sample to a degree reflected by the maximum current flowing through the sample. The new $I-V$ characteristics of a formed sample exhibit currents larger by a factor $\simeq 10^8$ than the unformed sample[132]. If, however, the voltage exceeds V_F, the degree of forming may increase further, providing V_F does not exceed a certain final forming voltage which will cause catastrophic breakdown of the insulator[133]. The rate of the forming process is very sensitive to temperature. In general, if the temperature is high enough, the sample will form to completion at a faster rate than it does at a lower temperature. At a particular value of V_F, the device may continue to form if the temperature is increased without any change in V_F. However, the degree of forming is constant at given T_F (forming temperature) and V_F (final) providing the latter is not further increased. It has been shown that the forming voltage is apparently independent of the insulator thickness[132]. Nevertheless, the degree of forming does depend on the thickness d, and the peak current of a formed device is approximately given by[133]:

$$I_{max} \propto d^{-3}.$$

Since the degree of forming is sensitive to the peak current this, in turn, should also depend on thickness. In fact, the degree of forming decreases with increasing thickness. The thickness range of the insulators suitable for the forming process is regarded to lie between 100 Å–3000 Å. As already indicated for a thin insulator, V_F may exceed the breakdown field, and the probability of electrode-electrode tunnelling becomes significant. A decrease in peak current is observed with increasing insulator thickness[133].

The forming process is found to occur under varying vacuum conditions, for instance, pressure of 1 Torr or lower was found to be adequate by Hickmott[135,136], 10^{-5} to 10^{-8} Torr was found necessary in the investigations by Barriac *et al.*[137–139] who also reported that no forming occurs at 10^{-3} or above. The widely accepted pressure, however, is 10^{-2} Torr or better. This process is not affected too much if gases like He, Ne, H_2, Ar are used instead. However, an oxygen atmosphere completely inhibits forming and may have permanent effects. The forming process was investigated using a wide variety of electrode materials such as Al, Au, Ta, Zr, Ag, etc., with different combinations of counter-electrodes. Different behaviour of the device has been exhibited with different polarity of the electrodes. Behaviour is dependent upon anode material, to which forming is sensitive, but not upon the cathode material.

Dearnley *et al.*[132] have tabulated different electrode materials based on experimental observations, and have shown which of these exhibit forming under different conditions.

7.2 *Models of the Forming Process*

Since Hickmott[135,136] pronounced the occurrence of "forming" in MIM devices and proposed a model to explain the observed behaviour of the device, many more models have been developed. Each of these explained the "forming" and consequent changes in the device characteristics in a somewhat different manner. However, none of these models accounts fully for the numerous observations demonstrated in different devices. To remind the reader of the very basic concepts of these various models, we reproduce a concise summary of all five models in a

TABLE III
Summary of the models to explain the "forming" process in insulators [After Dearnley *et al.*[132]].

Author	Model proposed	Local or general forming	Dependence on electrode	Dependence on insulator	Dependence on atmosphere
Hickmott	Schottky ionization of impurities near middle of bandgap; formation of localized states for impurity band and space charge to aid injection of electrons	Uncertain	No detailed model; probably depends on work function	$V_F \simeq$ ½(energy gap); voltage-dependent since ionization of impurities is so	No detailed model; probably impurity–oxygen reaction
Simmons–Verderber	Injection of ions from anode to form broad impurity band with a sharp top. Band bending from space charge	Not local	Impurity levels depend on species; band bending depends also on work function	V_F usually less than ½(energy gap); depends on electrode, through impurity levels. Voltage-dependent because impurity spectrum and bandgap fix V_F	Apparently none since the injected ions do not react strongly with oxygen
Dearnley	Propagation of conducting filament through film	Local	Forming initiated at anode and can be inhibited if electrolytically released gas reacts readily with anode	V_F probably related to crystal formation energy or to breakdown strength. Voltage-dependent because forming initiated in small region	Oxygen causes competing reactions which prevent filament propagation or initiation
Barriac *et al.*	Local fusion of insulator and electrode, with subsequent ion injection. Also traps formed	Probably not local	Not discussed	Not discussed	Oxygen neutralizes the ions which constitute the space charge
Greene *et al.*	High-field electrolysis with injection of vacancies from cathode	Probably local	If the anode reacts readily with gas released, growth of insulator at anode may inhibit forming	$V_F \simeq$ Gibbs free energy of formation of insulator	Oxygen causes other competing reactions at cathode

tabular form (Table III), after Dearnley *et al.*[132]. More discussion will follow when the experimental observations on Langmuir films are described later in this section.

Once the device is "formed" many electrical phenomena can be observed, which an unformed device does not exhibit. The most commonly observed phenomena are DNR together with switching and memory phenomena. In some structures, however, electroluminescence and electron emission may also occur. Since Langmuir films exhibit only DNR in the experiments on diode structures (MIM) and triode structures (MIMIM), we shall discuss briefly how the DNR can be explained in terms of various models. The other observed phenomena, described in an earlier review[132], will not be included in the present paper. Further, we shall limit our discussion to the voltage controlled (N-type) DNR which has been observed in Langmuir films.

The earliest model proposed by Hickmott[135,136] states that the initial part of the $I-V$ characteristic is due to space-charge limited conduction in the impurity band of the insulator. When a high field is applied, some process reduces the number of impurity centres, which in turn reduces the conductivity, and an N-type characteristic results. For

instance, neutralization of the impurity centres by field induced inter-impurity tunnelling may be one possible process to cause this reduction of conductivity. In another model[134], the electron transport mechanism has been assumed to be hopping between traps of very similar energies when the applied voltage exceeds a particular limit ϕ_I, below which electron tunnelling from one electrode to another is probable. At high voltages ($>\phi_I$), the insulator can be crossed only by those electrons which are entering the insulator with energies close to the electrode Fermi energy, and only if they are making transition to traps of lower energy. Since the top of the impurity band in the centre of the insulator has been assumed to fall below the anode Fermi level, charge trapping would occur in the depletion layer near the anode. The density of states of electrons within the electrode decreases, resulting in a rapid fall of the number of electrons contributing to conduction, and thus giving rise to the negative resistance in the characteristic. In a model by Barriac and co-workers[136–139] non-ohmic behaviour at low voltage has been attributed to space-charge limited ionic currents. They have thus introduced an additional feature of ionic motion unlike the previous models of Hickmott[135,136] and Simmons–Verderber[134]. At higher voltages, the dominant transport mechanism has been suggested to be electron tunnelling, which neutralizes the positive ionic space charge by being trapped. Consequently, the two current-carrying components are largely cancelled, and an N-type characteristic results.

A model based on an altogether different approach involving some conducting filament formation in the device has been proposed by Dearnley[140]. Basically, the model assumes ohmic conduction along the filaments which are physically different from the host matrix. The appearance of negative resistance has been attributed to the rupture of these filaments due to Joule heating to a point exceeding the melting point of the matrix. On fracture, the filament becomes non-conducting, resulting in the fall in conductivity. An earlier model[141], having features in common with Dearnley's model, postulates only one filament, and explains the occurrence of switching in the device but no negative resistance. One of the recent models by Sutherland[142] is similar to that of Dearnley *et al.*[132] and this also assumes that the DNR arises from local breaking of thin conducting filaments by Joule heating. Thus, all these models propose diverse mechanisms for DNR. It will be shown later in this section which of these offer interpretation to the observations in Langmuir films.

7.3 Experimental Observations on Langmuir Films

Experiments were performed both on diode structures[130], (metal-organic film-metal) and triode structures[131] (metal-film-metal-film-metal) using Al electrodes and organic films of cadmium arachidate. The unformed samples were placed in a sealed brass box evacuated to 10^{-3} Torr whose temperature could be varied between 77°K and room temperature. Then a unipolar sawtooth voltage, which increased at 0.3 V sec^{-1} and decreased to zero within 0.02 sec, was applied across the devices. The J–U characteristics do not manifest DNR in the return trace if the voltage is removed this quickly[132,134]. The measurements on diodes have used 11-layer thick films, and on triodes 9-layer thick films. In the case of diodes, characteristics are also obtained with Au as the upper electrode to explore the influence of electrode material on the characteristics. Some devices with Au as the base electrode were prepared which invariably showed short circuits as was reported by Handy and Scala[42].

7.3.1 DNR on Diode Structures Once the sample is "formed" at 77°K with top Al electrode positive, typical J–U characteristics are obtained, similar to that shown in Figure 29 for a sample consisting of 11 organic monolayers. As a rule, DNR is not observed in the first voltage cycle but appears in the second one. However, it disappears in the successive two to four further cycles and finally the characteristic becomes smooth. Figure 29 at 77°K corresponds to this smooth characteristic. On warming up of the device at about 5°K/min, the J–U characteristic changes at about 150°K and behaves at different temperatures as shown in Figure 29. Evidently, the most pronounced DNR (peak to valley ratio of the current is maximum) is observed at about 190°K and it goes on diminishing beyond this voltage, disappearing above about 210°K. Similar results were obtained with Au top electrode but the device always exhibited short circuit above about 170°K, and in this case appreciable DNR occurred at about 150°K.

To investigate the temperature effects, the unformed sample was always cooled to 100°K and sawtooth voltage applied until the device exhibited smooth characteristics. In Figure 30, curves 1, 2 and 3 represent the respective characteristics of an unformed sample in the first voltage cycle; of a formed sample in the second voltage cycle exhibiting DNR; and a smooth characteristic after a few voltage cycles. The device was then treated at a particular

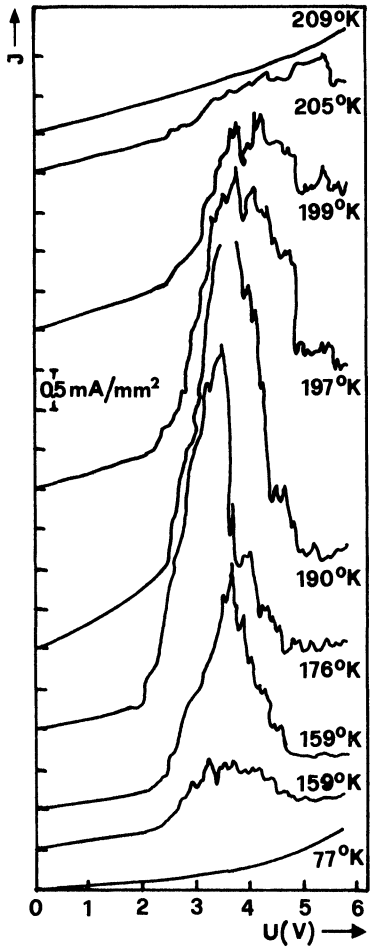

FIGURE 29 Current-voltage characteristics of an Al-(Al-oxide)-11 monolayers-Al sandwich for increasing temperature, top electrode being positive. The vertical scale is displaced for each curve for clarity. DNR completely disappears above about 210°K. [After Gundlach and Kadlec[130].]

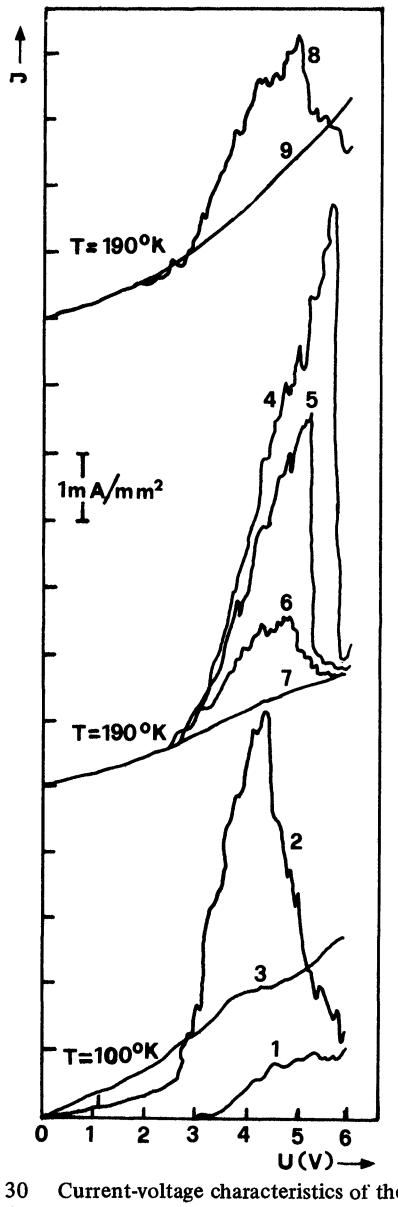

FIGURE 30 Current-voltage characteristics of the device as in Figure 29 at different voltage cycles. Curve 1: first voltage cycle of an unformed sample. Curve 2: second voltage cycle; the sample is now formed and exhibits DNR. Curve 3: smooth characteristic after a few voltage cycles; sample temperature was 100°K. Curves 4 to 7: first four voltage cycles after temperature increases from 100°K to 190°K. Curve 8: first voltage cycle after interrupting junction bias for 3 hours, at 190°K. [After Gundlach and Kadlec[130].]

temperature in the range (110°K–300°K) and each time the voltage was removed while raising the temperature. DNR was observed only for the first few voltage cycles in systematic studies of different temperature regions. The typical curves so obtained are shown by the curves 4 to 7 in Figure 30. The observations made in different temperature ranges are:

a) 110°K–150°K; exhibited DNR but not well pronounced.

b) 150°–190°K; better DNR than above.

c) 190°K–225°K; pronounced DNR (see curve 4 of Figure 30).

d) 225°K–300°K; increase in conductivity; little or no DNR.

It was also observed that the current maxima shifted towards lower voltages with increasing number of voltage cycles until the DNR disappeared. However, it could be re-obtained by increasing the temperature in the range 100 to 225°K. Thus, it was found that the larger the temperature increase, the better the DNR is developed. Curve 8 in Figure 30 illustrates a characteristic at 190°K, which the device exhibited in the first voltage cycle after interrupting the voltage bias for about 3 hours. The DNR is more pronounced for longer resting times. Curve 9 shows a smooth characteristic obtained after a few more voltage cycles at 190°K after interruption as in curve 8. Further experimental observations concerning DNR in diode structures by Gundlach and Kadlec[130] may be summarized as below.

a) The device could be formed by applying 5 to 6 V or more when the top electrode (Al or Au) was biased positively. The temperature at which the device "formed" was 77°K unlike in the case of many oxides and insulators ($T \simeq 200$°K for Al–SiO–Au[133] and $T \simeq 250$°K for Al–Al oxide–Au[130]). This has been explained in terms of the very weak binding forces between continuous hydrocarbon chains oriented perpendicular to the film plane of the insulator. In contrast to oxides which do not have such an anisotropy in binding forces, the mobility of impurity ions (here metal ions) along the long chains of the molecules is expected to be higher than in oxides. To explain the fact that the device cannot be formed (at 77°K) when the base electrode is positive, a qualitative suggestion has been made that the thin Al oxide film (formed between the lower Al electrode and the Langmuir film) inhibits the metal ion injection from the base electrode into the organic layers.

b) Once the device is formed, the DNR is observed for both polarities of voltage bias. The threshold voltage for the appearance of DNR was found to lie between 2 and 3 V.

c) The investigations of DNR with respect to the multilayer thickness showed that the former becomes more pronounced with the increase of the latter. The average values determined[130] for the peak-to-valley ratios from the observations of 35 samples, were 4.2, 2.1 and 1.45 for 11, 9 and 7 monolayers, respectively. No DNR was observed for devices having less than 5 monolayers. Gundlach and Kadlec[130] were not able to explain this behaviour.

To explain the existence of DNR, no single theory was found adequate. However, the appearance of DNR below 225°K (see Figure 29) has been related to the so-called "dead time", which is a measure of the time between filament fracture and reaching a state from which it may reform[132]. In this model[132] the transition between two states is interpreted as relaxation of space charge polarization. On the other hand, the dead time is related to electron diffusion through the insulator[134,143]. However, both of these models predict a strong increase of dead time with decreasing temperature. It has thus been suggested that these devices presumably show a dead time of the order of hours because DNR appears below 225°K. However things are not so simple, as the dead time has been reported to increase irreversibly from seconds to hours by warming Al–Al oxide–Au samples up to 500°K for about an hour[144]. Finally, the results have been left without an adequate explanation by the existing theories.

The peak voltage U_p was found to agree, within experimental error, with an empirical relation given by Hickmott[136], $U_p = 4 - 0.36\sqrt{\epsilon_r}$, when the device was warmed steadily (see Figure 29). For cadmium arachidate, the dielectric constant $\epsilon_r = 2.4$[53] was considered to obtain $U_p \simeq 3.45$. However, the values of U_p measured at constant temperature (Figure 30) are much higher. Therefore Gundlach and Kadlec[130] suggested that U_p cannot be related simply to band model parameters which assumes the constancy of U_p for the devices of the same material. Confirmation of this suggestion appears from the measurements on Au–ZnS–Au devices[142]. It has been shown that U_p can be increased drastically by applying voltage in the current minimum region of the characteristic for a period of up to a few minutes. In the model proposed[142], U_p is related to the distribution of filament resistance, which in turn depends on the spacing of positive centres in the conducting filament. To some extent, the observations of the present workers seem to be supported by the filamentary models which imply that the dead time and the voltage for current peak (U_p) can be changed for a given sample, but no satisfactory explanation exists. The disappearance of DNR above a certain temperature is also unexplained. Nevertheless, these observations have shown that low frequency DNR does occur in Langmuir films, and the phenomena under consideration are to a large extent independent of specific properties of the insulator material.

7.3.2 DNR on Triode Devices Hickmott[136] made the first attempt at studying this phenomenon in triode structures Al–(cathode)–

SiO–Al(grid)–SiO–Au(plate). Similar studies were also performed on aluminium oxide triodes[136]. Both the devices when "formed" showed that the potential distribution was highly non-linear between the plate-grid (V_{pg}) and grid-cathode (V_{gc}) regions. When DNR became fully pronounced, V_{pg} was proportional to V_{pc} and was rather small, whereas V_{gc} was nearly equal to V_{pc} (pc refers to plate-cathode region). On reversing the polarity of V_{pc}, the main voltage drop shifted to the plate-grid and then V_{cg} was nearly proportional to J_{cp}. [In the discussion V_{pc}, J_{pc}, V_{pg} and V_{gc} refer to plate positive and V_{cp}, J_{cp}, V_{gp} and V_{cg} to plate negative.] Hickmott, however, could not satisfactorily explain these phenomena in triodes.

Gundlach and Kadlec[131] after a successful attempt to study the DNR in diode structures (discussed above), extended their studies to triodes by making use of organic monolayers and following the arrangement and circuitry, etc., of Hickmott[136]. However, all three electrodes used were of aluminium to avoid unnecessary asymmetry. The grid, of thickness ≃50 Å, contained a significant number of pin-holes and the other two electrodes (plate and cathode) were several thousand Å thick. The device was formed at 77°K as in the case of diodes; DNR was found to occur in the second voltage cycle and to disappear in the next few cycles. At about 170°K, the DNR was more pronounced and V_{pg} and V_{gc} changed little as compared with that at 77°K (V_{pc} was equally divided between V_{pg} and V_{gc} at 77°K). In Figure 31, the $J_{pc} - V_{pc}$ characteristic at 170°K and the changes of V_{pg} and V_{gc} with respect to V_{pc} are shown. Evidently, both V_{pg} and V_{gc} increase nearly proportionally to V_{pc} but these are independent of the $J_{pc} - V_{pc}$ characteristics. The explanation offered for the latter observation is in terms of the filamentary model of Dearnley *et al.*[132], according to which DNR occurs by filament breaking because the fractured filament does not contribute to the current. After the so-called dead time, the filament may reform, which presumably occurs at about 2.8 V in the present case (see Figure 31). It has been assumed that the current J_{pc} flows along the conducting filaments which cross the grid at pin-holes.

Further warming up of the triodes results in a drastic change in the $J_{pc} - V_{pc}$ characteristic as well as in the voltage distributions V_{pg} and V_{gc}. At about 230°K, the DNR disappears (see Figure 32) which is typical for organic multilayer triodes. A slight non-linearity in the characteristic is observed in the plate-grid region; the spike σ, however, originates in the grid-cathode region. The dotted curve in

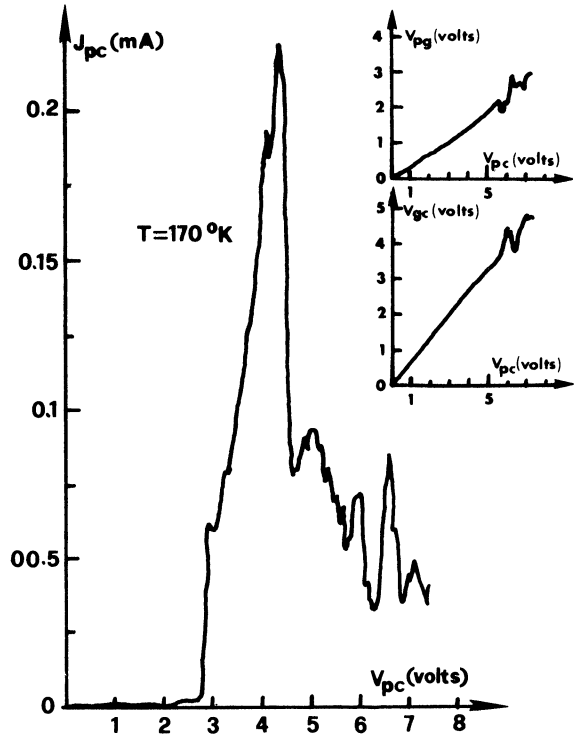

FIGURE 31 Current-voltage characteristic and voltage distribution of an Al-9 monolayer-Al device at 170°K, the plate being positive. [After Gundlach and Kadlec[131].]

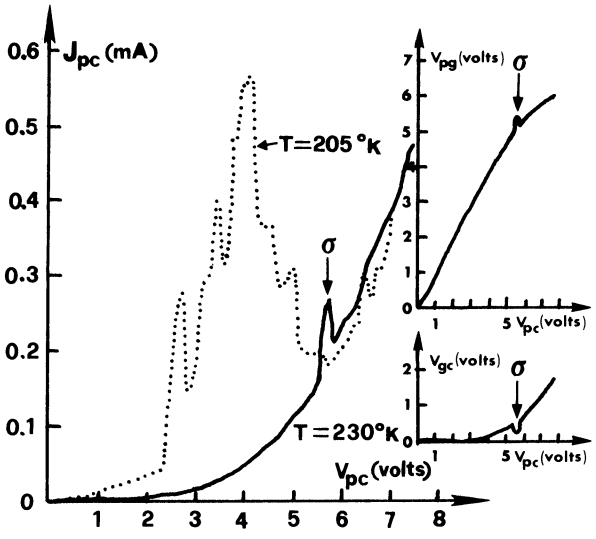

FIGURE 32 Current-voltage characteristic (full curve) and voltage distribution of the device similar to that in Figure 31 at 230°K. The dotted curve is J–V characteristic at 205°K. The spike σ in the curves is probably just a consequence of new events at 230°K. [After Gundlach and Kadlec[131].]

Figure 32 is a $J_{pc} - V_{pc}$ characteristic at 205°K, which has been considered to represent the sum of two types of currents below 5.5 V. The first is slightly non-linear without showing DNR and the other showing DNR which ceases at 230°K. Non-occurrence of DNR above a certain temperature, and hence the disappearance of the current associated with DNR has been interpreted by assuming that either the filament does not reform or it needs rather a long time to do so. The presence of spike σ and the slightly higher current above 5.5 V have been attributed merely to some new events occurring at 230°K. Nothing in particular has been stated about these new events.

After a sufficient number of voltage cycles, the voltage V_{pg} or V_{gc} was found to be generally proportional to J_{pc}; unlike that shown by the dotted curve in Figure 32. Reversing the junction bias at 270°K (plate negative) led to an increase in V_{cp} from 7.5 V to 9.5 V, which resulted in higher current J_{cp} (than J_{pc}) and, therefore, a changed $J_{cp} - V_{cp}$ characteristic. On the other hand, V_{cg} decreased considerably but was still proportional to J_{cp}. One remarkable feature is that Gundlach and Kadlec[131] also succeeded in developing the main voltage drop in the grid-cathode region when V_{pg} was proportional to J_{pc}. This was not reported in the earlier experiments on oxide triodes[136]. Thus, it has been concluded that there is no region in the monolayer triodes which exhibits preferential DNR and it might be due to the electrode symmetry of these triodes. Resistances R_{pg} and R_{gc} of a formed device (measured at 0.3 V) were found to be 1 to 2 orders of magnitude higher than R_{pc}, which resembled the observations on SiO triodes[136].

In both the experiments on diodes and triodes, Gundlach and Kadlec have explained the observations qualitatively in terms of the filamentary models; nevertheless, they have remarked that the model itself is still speculative. With the use of Langmuir films as the insulator, some typical observations, e.g. the device formation at 77°K, the dependence of DNR on the film thickness and disappearance of DNR above a certain temperature, are yet to be interpreted. Therefore, the immediate requirement is the development of a new model, essentially based on filamentary models which could partly explain the DNR phenomena in these films. One suggestion of Gundlach and Kadlec,[131] that the thin oxide film (between the base electrode and the organic multilayer) inhibits the injection of metal ions from the base electrode into the organic layers, does not appear to be convincing.

In the recent work[63] on thermally stimulated currents in such organic layers, the device used was Al–film–Al and the ion displacement from one electrode to the other has been shown to form an ionic space charge which is responsible for the polarization. Particularly in future works, the possibility of the occurrence of several other phenomena, like switching and memory, which have already been observed in a wide variety of oxides, must be ascertained for Langmuir films. This might seem to be a speculation at the first instance, but the reader must remember that even DNR was never thought to occur in these monolayers before Gundlach and Kadlec made a successful study. At least, the studies of DNR have shown that such a phenomenon is not restricted to insulators of a particular chemical composition and crystal structure. More investigations on DNR occurrence must also be carried out using different types of organic films sandwiched between varying metal electrodes to ascertain the influence of the electrode material on "forming" processes, and to strengthen the proof of DNR in these insulating materials.

8 IONIC TRANSPORT PHENOMENA IN LANGMUIR FILMS

The study of ionic polarization and transport in many insulating materials has been pursued by workers engaged in thin film investigations. Such studies were reported by Curie[145] as early as 1886 on quartz crystals, and subsequently Warburg and Togetmeier[146] demonstrated the steady-state transport of ions such as Na^+, Li^+ and K^+ through quartz at temperatures below 250°C. Since then, ionic motion has been shown to occur in a wide range of insulating or semiconducting materials and the subject has developed considerably.

In recent years, some problems of commercial importance, for instance the surface stability of MOS structures for reliable operation, have been associated with the motion of ions within the oxide layer on the semiconductor surface, and therefore, the necessity of such studies were realized. The change in the capacitance-voltage characteristics of MIS structures has been suggested to provide a powerful tool for the observation of ionic motion in thin insulating films. Similarly, the method of measuring ionic thermocurrents[147] is known to be a more sensitive method to investigate polarization effects due to ionic motion in insulators. It has been shown that this method reveals finer details of the phenomena than the two

earlier methods in use, i.e. by considering the change with time of the electrical current in a device subjected to a dc external field[148,149] and by measuring the dielectric losses[150,151].

Fortunately, in recent years some workers have made successful attempts to study Langmuir films in the form of MIM and MIS structures to determine the polarization effects and $C-V$ characteristics with respective structures. Here we shall mainly be concerned with the discussion of such studies on Langmuir films. Preliminary data obtained on change of capacitance with applied voltage on these films will also be given in this section.

8.1 Properties of MIS Structures

The study of capacitance-voltage characteristics in MOS structures has proved to be of potential importance in developing certain types of devices. To investigate the usefulness of Langmuir films for such devices, Tanguy[152] carried out studies on MIS structures using the organic films of Ca-behenate and orthophenanthroline with three stearate chains. The p-type silicon surface after etching in CP_4, cleaning and drying, were used with deposited organic multi-layers, and were then covered by aluminium in the form of two circles connected by a channel which served as the top contact. The back contacts were of evaporated gold or of an Au–Si eutectic. To know the thickness for one monolayer of orthophenanthroline, measurements of the device capacitance C were made with respect to the number of monolayers N deposited. The linear relation between $1/C$ and N thus gave a monolayer thickness of about 15 Å. All the capacitance measurements were performed on a General Radio 1620 A bridge under low pressure for good reproducibility of the results. Figure 33 shows the $C-V$ curves obtained with 3, 5 and 9 monolayers of orthophenanthroline in which both accumulation and inversion regions are visible. Evidently, even a small variation in bias voltage results in a large modulation of C, which has been thought to arise from the small thickness of the insulator and from the high resistivity ($\simeq$600 Ω cm) of the p-type silicon. The curves shown in Figure 33 represent the situation a short time after etching. In the case when silicon was left for a few hours in the ambient conditions before monolayer deposition, the flat band voltages shifted towards the positive charge, and the slope of the curve was found to become less steep than shown in Figure 33. When the aluminium top electrode was replaced by gold, the flat band voltage shifted to zero and the distance between the flat band voltages of both curves corresponded to the difference between the respective work functions.

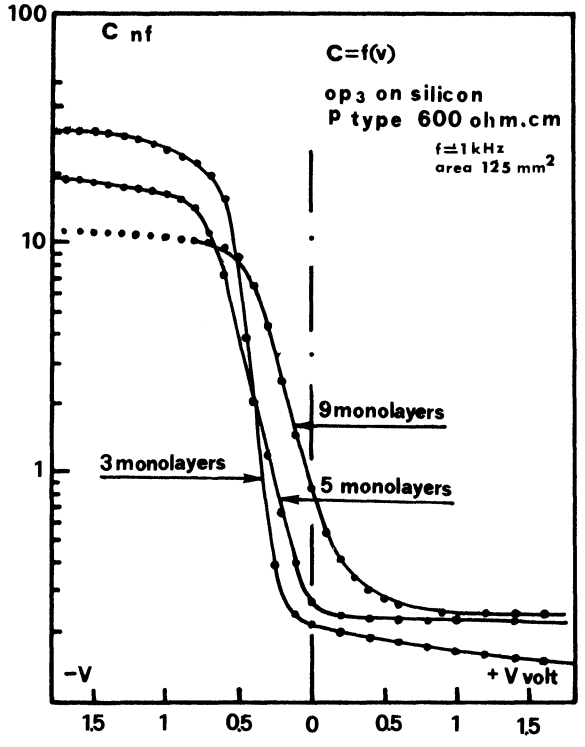

FIGURE 33 C–V curves for MIS structures (area $\simeq$ 125 mm²) with 3, 5 and 9 monolayers of orthophenanthroline at a frequency of 1kHz. [After Tanguy[152].]

In several studies[153–156] on MOS structures, the two types of hysteresis, normal and abnormal, are attributed to the ion displacements in the insulator and to the trapping at interface states. Tanguy[152] also obtained both types of hysteresis (shown in Figure 34). Figure 34 shows $C-V$ curves of 5-layer thick orthophenanthroline (OP_3) device at various temperatures. The normal hysteresis is related to V_{FB} (flat band voltage) shift opposite to the voltage bias, whereas the abnormal one is characterized by V_{FB} displacement towards the bias voltage. In accordance with the earlier workers, Tanguy has also tried to correlate the existence of these two hystereses with ionic motion in the insulator and trapping, respectively. Presence of ions in the fatty acid soaps is a well known feature, as these are ionic substances forming stable monolayers (Ref. 7, p. 193) and there is a possibility that some ion content might get transferred during monolayer deposition. Frequently, ions can be adsorbed later during electrode evaporation. Tanguy has, however, made use of the novel tech-

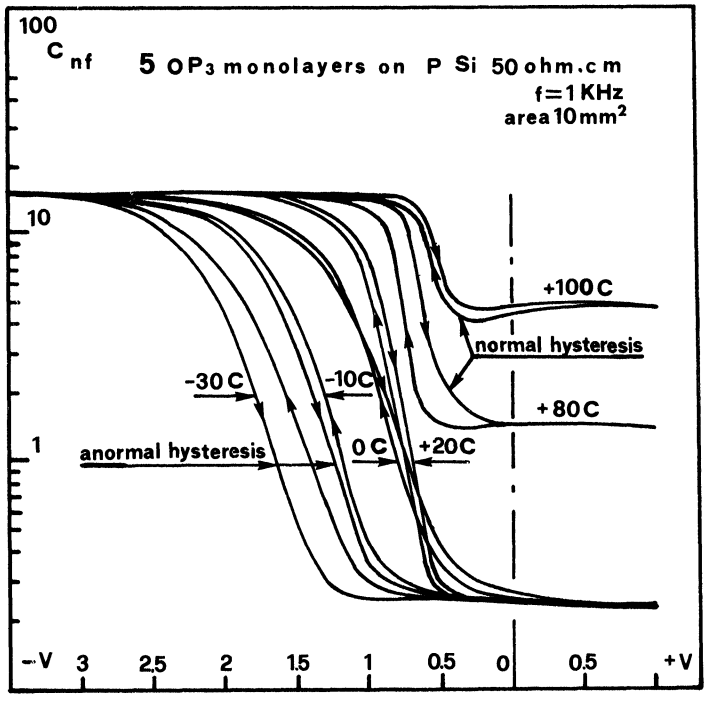

FIGURE 34 Shift of C–V curves with 5 OP_3 monolayers deposited on p-type silicon as a function of temperature. The area of MIS device was 10 mm^2 and measurements taken at f = 1kHz. Normal and abnormal type of hystereses are indicated. [After Tanguy[152].]

nique of studying thermally stimulated currents (TSC) in these organic films to make sure of such ionic motion. TSC measurements were performed on MIM structures with one layer of OP_3. These experiments gave a clear-cut indication that the short circuit currents arising on warming up of the structure are a consequence of ion displacements because the amplitude of the current peaks varied greatly with the bias temperature. At lower temperatures, such peaks were not observed. Further, it was estimated from TSC peaks at 20°C that about 2×10^{10} charges are displaced or trapped, which corresponds to a $C-V$ curve shift of the order of 100 mV for 3 OP_3 monolayers. To make sure of this statement, $C-V$ curves were obtained for 3 OP_3 monolayers with different temperature bias conditions which yielded V_{FB} shifts agreeing quite well with the above estimation. This estimation assumes that the mobile ions can move from one electrode to another. In a separate measurement of TSC in calcium behenate monolayers, it was found that the number of free ions is less important, which has been attributed to the fact that stearic acid chains are more compact in behenate than in OP_3.

Abnormal hysteresis, which appears below 20°C in the case of OP_3 (see Figure 34), has been found to become very important for calcium behenate. In the latter case, a continuous V_{FB} shift extending to about 1 V in an hour has been observed. To explain the existence of abnormal hysteresis, Tanguy assumed that the traps occur in the natural oxide layer. However, it could not be proved in these preliminary investigations that no trapping exists in molecular layers. In one of the models[155] proposed to explain the abnormal hysteresis in MOS structures, it has been assumed that the holes emitted from the valence band of the silicon are trapped in the oxide or at the interface, and these positive charges cause V_{FB} shift towards negative voltage. Some workers[157] found a correlation between the number of charges in the oxide layer and the number of surface states in the silicon. This has been regarded as an explanation of the observed instabilities with the calcium salt in the present investigations.

In an earlier communication, Tanguy and coworkers[45] reported $I-V$ characteristics on MIM structures using OP_3 as an insulator. When similar experiments were repeated on MIS structures by

Tanguy, the currents observed were in good agreement with those obtained for MIM structures. It has been found however, that the currents are weak compared with those obtained from MOS structures[158] with the oxide of comparable thickness. Figure 35 shows the $I-V$ curves for MIS structures

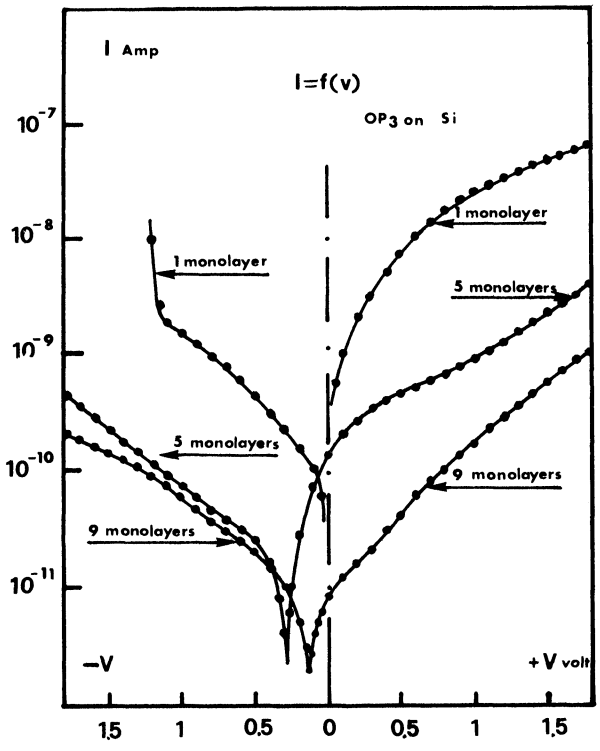

FIGURE 35 Current-voltage characteristics of MIS devices with different number of OP_3 monolayers deposited on Si. Notice the shift of I–V curves near zero V indicating the existence of an emf without external bias. [After Tanguy[152].]

obtained on 1, 5 and 9 monolayers of OP_3. Evidently, there is a shift of $I-V$ curves near zero V which reveals the existence of an electromotive force in the monolayers when there is no external bias. It has been suggested by Tanguy that the emf arises, presumably, from chemical reactions in the layer at the interface. In an earlier work by Leger *et al.*[55], the existence of emf in MIM structures was reported. It was found that the junctions act as batteries because a voltage of about 200 mV was obtained when a high impedance voltmeter was connected across the junctions. The existence of emf has been suggested as arising due to the motion of charged ions across the insulator to attain the equilibrium state. These workers could not comment on what type of ions actually cross the molecules, but some kinetics of these ions have been studied in the range 20°–70°C. For instance, the internal resistance $R_{int} \propto \exp(E_0/kT)$ where $E_0(\simeq 0.36$ eV) is the activation energy, which is comparable with the activation energy (0.6 eV) required for water molecules to cross a fatty acid monolayer spread on water surface to prevent its evaporation[159]. It has also been noticed that the initial emf of the battery depends on the nature of the sample under investigation, but E_0 remains the same. To realize the practical importance of observed emf in these junctions, 226 junctions of 0.25 mm^2 each were prepared and connected in series. The values obtained for total voltage was 50 V, $R_{int} \simeq 10^{10}\ \Omega$ and the total volume of MIM structures $\simeq 0.1\ mm^3$. It has been thus suggested that such a high impedance battery with so small a volume might prove of special significance in a few practical applications. The capacity of these cells ($\simeq 1\ \mu C$) has been found to correspond to the oxidation of about one atomic layer.

One of the most significant contributions of Tanguy[152] has been in obtaining the reproducible MIS structures which behaved almost as MOS structures. This has opened up a new field of investigations for studying semi-conductor surfaces using organic molecules which might be exposed to high electric fields. In these basic investigations, occurrence of abnormal hysteresis in MIS structures could not be explained very well, and therefore further studies with other types of organic molecules are needed for a better understanding of the phenomenon. Technological applications of MIS devices, like those of MOS devices, must also be worked out after successful studies on MIS structure.

8.2 Thermally Stimulated Currents

The ionic thermoconductivity method[147,160], which involves the study of the thermal activated release of dielectric polarization has already been used in a wide variety of dielectrics. The essential steps of the method are: (i) Polarization of the sample in a static field E_p at the temperature T_p for a time t_p. The temperature should not be too high to develop heavy space-charge. (ii) The sample is then cooled down to a temperature $T_0 \ll T_p$ so that the relaxation time $\tau(T_0)$ is of the order of several hours or longer. (iii) The electric field E_p is now turned off (at $T = T_0$) and the dielectric is warmed up with a constant rate $\beta = dT/dt$ and the discharge current is registered as a function of temperature. The polar-

ization current $i(T)$ first increases exponentially, reaches a maximum and then drops to zero. Thus the analysis of the peak obtained allows the determination of the activation energy of the relaxation process and reveals the finer details of polarization.

Tanguy[152] initially used this method on Al–orthophenanthroline–Al structures to observe ion displacements in monomolecular films. Such studies were carried out to explain the normal hysteresis in MIS structures and it was stated that the mobile ions in the monolayers can move from one electrode to another. In the structures studied, ion displacement was held responsible for the large variation in the amplitude of the current peaks at higher temperatures. Later on, Tanguy and Hesto[63] have made a systematic study of the polarization phenomena in MIM structures by thermally stimulated currents (henceforth TSC) method. We shall first discuss the theory used by these workers to explain TSC in organic films and then the experimental observations will be described.

8.2.1 Theoretical Model Of all the models, the one found suitable to explain the TSC peaks assumes that the electrical charges can move between two potential wells separated by only a few Å. In this model the charge contained by the two potential wells changes when the device is subjected to an applied field, and gives rise to a volume polarization called "orientational polarization" in the specimen. The position and shape of the TSC peaks thus obtained depend only on the potential barrier height and not on the initial experimental conditions (temperature, electric field, polarizing time) as in the other theories[161].

Assuming N pairs of potential wells per unit volume which are randomly distributed, and if $2a$ is the separation between two centres, the total polarization P_i is given by[162]:

$$P_i = eaN \int_0^1 Z \tanh(uZ)\mathrm{d}Z, \tag{8.1}$$

where

$$u = \frac{eaE_p}{kT_p}$$

If the electric field E_p is relatively small, then $u \ll 1$ and Eq. (8.1) reduces to

$$P_i = \frac{N(ea)^2 E_p}{3kT_p} \tag{8.2}$$

which shows that polarization is a linear function of the applied field E_p. Further, the relaxation time τ which is the average time needed by a charge to hop from one position to another over a potential barrier ϵ, has been defined as

$$\tau = \tau_0 \exp\frac{\epsilon}{kT}, \tag{8.3}$$

where τ_0 is a constant.

The initial polarization is a function of the polarization time t_p during which the sample is held at the initial temperature T_0 (room temperature) according to

$$P_0 = P_i(1 - \mathrm{e}^{-t_p/\tau}). \tag{8.4}$$

If a MIM device is then cooled rapidly to 77°K, it releases the stored charge on reheating so that the discharge short current may be expressed as

$$J(t) = -\frac{\mathrm{d}P}{\mathrm{d}t} = -\frac{P}{\tau} \tag{8.5}$$

where P is the deviation of polarization from equilibrium.

If the reheating is a linear function of time, $T = T_0 + \beta t$, where β is a constant, the discharge current as a function of temperature can be written as (using expressions (8.3) and (8.5)):

$$J(T) = \frac{P_0}{\tau_0} \exp\left\{-\frac{\epsilon}{kT} - \frac{1}{\beta\tau_0}\int_{T_0}^{T} \exp\frac{-\epsilon}{kT}\,\mathrm{d}T\right\} \tag{8.6}$$

This polarization current gives a maximum at $T = T_m$ and its derivative at $T = T_m$ presents a relation between T_m, ϵ and τ_0 expressed as:

$$\tau_0 = \frac{kT_m^2}{\beta\epsilon \exp\dfrac{\epsilon}{kT_m}} \tag{8.7}$$

Clearly, from Eqs. (8.6) and (8.7), the shape of TSC depends only on the parameter ϵ and the maximum peak amplitude depends only on P_0. In their work, these authors have fitted the experimental peaks on the theoretical curves of Eq. (8.6) and determined the polarization parameters ϵ and τ_0. Separate values of N and a have also been calculated by fitting the experimental curves of P_0 as a function of the electric field in the theoretical curves obtained from Eq. (8.1).

8.2.2 Experimental Measurements Tanguy and Hesto[63] tried to obtain data under various experimental conditions, i.e. with varying temperature (T_p), voltage (V_p), time (t_p) and specimen thickness (d). In the measurements with respect to T_p on different

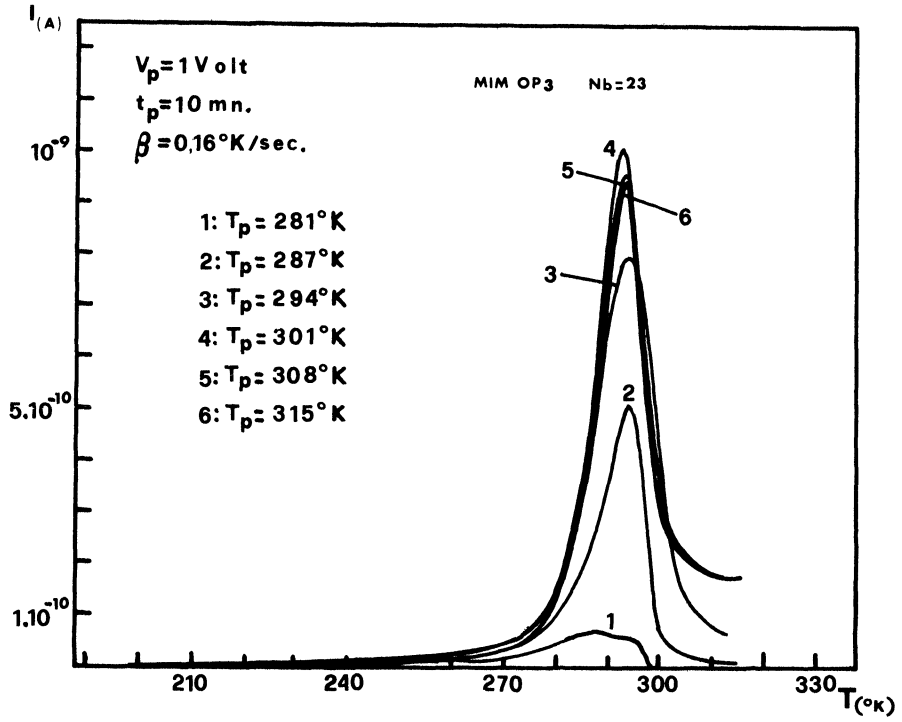

FIGURE 36 TSC peaks of a MIM device containing 23 monolayers of OP_3 at fixed $V_p = 1$ V $t_p = 10$ mn. and $\beta = 0.16°K/sec$. The peaks observed 1 to 6 correspond to various polarization temperatures $T_p = 281$, 287, 294, 301, 308 and 315°K. [After Tanguy and Hesto[63].]

numbers of monolayers of OP_3, the TSC peaks were found independent of T_p. Figure 36 gives a graphical representation of TSC peaks on 23 monolayers thick OP_3 at various temperatures ranging between 281°K to 315°K, when all other parameters V_p, t_p and β (rate of heating) were kept constant. Evidently, a polarization maximum is observed at $T_p = 301$°K, and there is a decrease beyond this temperature due to thermal agitation. This is clearly compatible with the theoretical expression (8.4) at high temperatures when τ becomes small and hence P_0 reaches a maximum. However, for $T_0 > 301$°K, the peak tail has been assumed to appear because of space charge formation. Since TSC peaks are well defined in position at room temperature, absence of space charge formation has been concluded.

When MIM structures were biased at different voltages V_p for a fixed time at fixed temperature, the TSC peaks obtained were perfectly stable. According to expression (8.1), P_0 must show a saturation at increasing electric field for $u > 1$, which these workers failed to obtain for 3-monolayer thick OP_3 structures because the applied field exceeded the dielectric breakdown ($\simeq 5 \times 10^6$ V cm^{-1}). However, on thick structures, such saturation was found to begin at $E_p = 10^6$ V cm^{-1} for 7 layers and $E_p = 4 \times 10^5$ V cm^{-1} for 21 layers. It thus appears that the applied electrical field sufficient to obtain maximum polarization depends upon the thickness of the film, which in turn increases a in the expression for u (see Eq. (8.1)). While studying P_0 as a function of polarization time t_p for 3 monolayers at 8°C, keeping the bias under 1.0 V, two distinct curves corresponding to $\tau_1 \cong 60$ sec. and $\tau_2 > 2000$ sec. were obtained. The former has been related to the charging time of lower energy peaks and the latter to the charging time of higher energy peaks. The time needed to form 80% of the total polarization was found to be ten minutes at 8°C and to reduce to one minute when the temperature was increased to 20°C.

Thickness-dependent studies of total polarization showed that the total polarization charge increases almost linearly with the number of monolayers Nb when T_p, t_p and E_p are held constant. Clearly, increasing Nb increases the value of a in Eq. (8.2) and thus the polarization charge increases because of the Na^2 term. According to this expression (8.2), the total polarization must not vary with increasing Nb

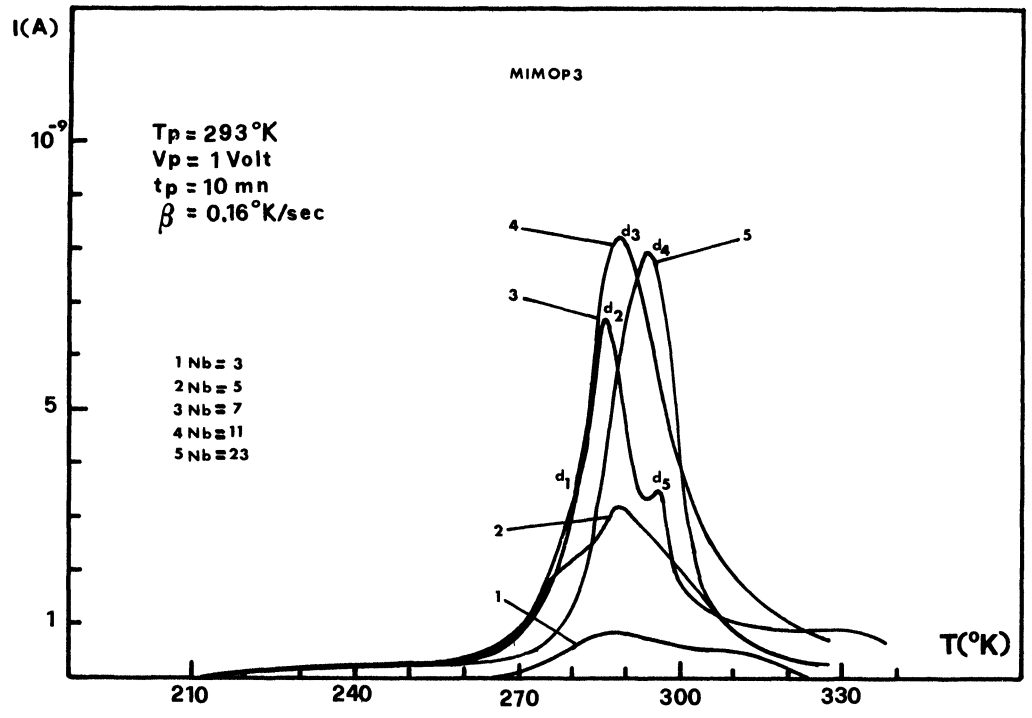

FIGURE 37 TSC peaks of a MIM device as a function of number of OP_3 monolayers at fixed $T_p = 293°K$, $V_p = 1$ V, $t_p = 10$ mn. and $\beta = 0.16°K/sec$. d peaks consisting of several mono-energetic peaks d_1, d_2, d_3, d_4 and d_5 are shown. [After Tanguy and Hesto[63].]

for a given electric field E_p because the number of potential wells N in the dielectric does not vary with the dielectric thickness. Since the basic structure of the monolayers changes with increasing dielectric thickness, the respective distance between two potential wells $2a$ and the activation energy ϵ are modified, resulting in the higher energy peaks of group d with increasing Nb. Figure 37 shows the TSC peaks obtained at different dielectric thicknesses when all other parameters were identical.

One of the important measurements carried out by these workers is the study of the influence of water molecules which, presumably, are adsorbed near the electrodes (possibly in the alumina). Initially, when a MIM structure was placed under low pressure and heated, a large space charge accumulation appeared and a broad peak with a maximum was obtained. This was the situation for temperatures beyond 60°C and when the dielectric thickness was relatively small. For higher thicknesses (≃23 monolayers), the space charge disappeared under low pressure at 30°C after approximately one hour. Conversely, the elimination of space charge needed about 48 hours for 3 monolayers and a few days for 1 monolayer. This has been qualitatively explained in terms of the influence of the electrodes on the electrical properties of the MIM device, which decreased with increasing dielectric thickness. It has been found that the polarization due to residual water molecules became negligible after a short stabilizing time of less than an hour at 30°C.

Tanguy and Hesto [63] further attempted to calculate the polarization parameters by fitting the experimental peaks to the theoretical curve according to Eq. (8.6). In their experimental investigations, several groups of peaks were identified, each characterized by a polarization temperature. In particular, they concentrated on d peaks, which are more pronounced in the case of multi-layers and are composed of several mono-energetic peaks d_1, d_2, d_3, d_4 and d_5 as shown in Figure 37. Since the polarization was found to depend greatly on the temperature and polarization time, these workers fitted two peaks obtained with 21 monolayers (see Figure 38) at temperatures of 290°K and 297°K and obtained the characterizing polarization parameters of all the d peaks. In another

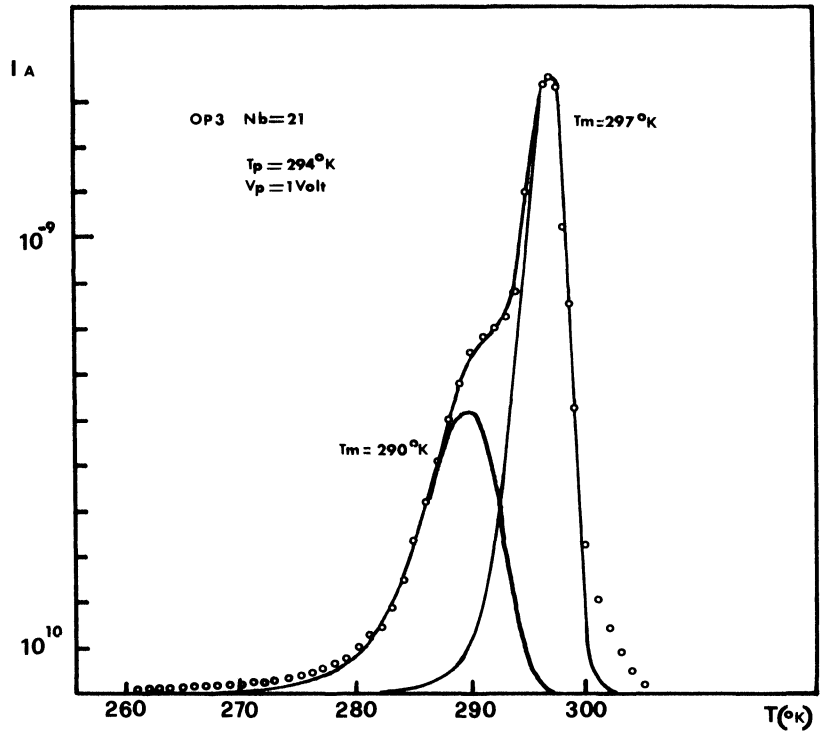

FIGURE 38 Typical curve fittings with 2 superimposed peaks for 21 monolayers of OP_3 at temperatures Tm = 290°K and Tm = 297°K. The solid lines in the figure represent theoretical fits and the circles are experimental points. [After Tanguy and Hesto[63].]

attempt, a fit of theoretical values of $P_0(E_p)$ (according to Eq. (8.1)) with the experimental curve for 21 monolayers was also obtained, and the parameters N and a were obtained for 3, 7, 21 and 170 monolayer-thick film structures. It has been reported that in depositing 170 monolayer thick films, OP_3 molecules dissolved in benzene were directly laid on the substrate and the solvent was allowed to evaporate. From these theoretical values, it was found that the polarization increases with increasing Nb, presumably due to an increase in the average distance $2a$ between two ion equilibrium positions. In fact, $2a$ has been found to increase from 1.2 Å for 3 monolayers to 10 Å for 27-monolayer thick structures. This phenomenon has thus been regarded as evidence for some basic structural changes in the multilayer with increasing thickness. From the calculated high values of activation energies ranging between 1.1 eV to 3.4 eV, and because P_0 varied rapidly with the polarization temperature, the hopping charges have been thought to be ions[163] which move between two equilibrium positions with $2a$ distance apart.

It has been discussed earlier that Marc and Messier[38] attributed the two absorption peaks to the dipolar movement in the amorphous and crystalline regions in the behenate monolayers (Part I, Section 4) and thus suggested some structural modification in these monolayers. Similarly, these workers[63] have assumed that as the monolayers grow thicker and thicker, the molecules tend to form crystallities whose number and volume increase with increasing film thickness. This assumption has been further justified by some experimental evidence. For instance they could also observe the structural modification optically by a colour change due to light reflection on the lower metallic electrode when the multilayers were heated to 35°C. At this temperature, presumably the CH_2 chain fuses, and OP_3 molecules are reordered forming crystallities. These crystalline regions in the multilayers have been assumed to be the trapping centres for the ions which are thermally released and can move in disordered regions, giving rise to the observed polarization phenomenon. It has been remarked further that calcium salts of stearic and behenic acid are of relatively low polarizability, especially when the chains are sufficiently long and

compact. In these cases, the polarization has been attributed more to an ionic space charge formation.

Whereas Tanguy and Hesto[63] have carried out a systematic and detailed study of polarization phenomenon in OP_3 molecules, a few points are not yet made very clear in their analysis. To the knowledge of the author, there is no other reported work in which the thick multilayers could have been obtained by simply laying the molecules, dissolved in solvent, on the substrate. It is rather surprising that these workers could form a uniform film in this simple way. Nevertheless, this simple method is fascinating and, in future work, specific attention must be paid to the suitability and applicability of this method to many other organic substances. Another remark must be made concerning the degree of structural modifications in behenate or stearate molecules and OP_3 molecules. According to Tanguy and Hesto,[63] the structural changes in the more compact behenate or stearate molecules are less evident, whereas Marc and Messier[38] have based all their experimental results on structural changes in these molecules. Therefore, structural studies have to be renewed and scrupulous attention must be devoted to this point. The role of metal electrodes, and of the oxide layer formed, must also be considered in future investigations.

8.3 Capacitance Studies with Applied Voltages

All the experimental investigations discussed in Section 4 relate to the capacitance studies of MIM structures as a function of monolayer numbers, which have also been employed by various workers as a simple tool to obtain monolayer thicknesses in the case of several organic compounds. Similarly, Leger *et al.*[55] obtained the thickness of a stearate monolayer, about 22 Å. These workers further studied the variation of capacitance of MIM structures as a function of applied voltage V and obtained some useful information. Figure 39A represents plots of $\Delta C/C$ (where ΔC is the change in the capacitance) versus applied voltage V on Al–barium stearate–Al samples with the capacitor area $\simeq 0.25\ mm^2$, for a varying number of layers. Clearly, the nature of the curve varies with the number of deposited monolayers, and all the data can be fitted to obey the universal linear dependence of the type $\Delta C/C = AE^2$ (shown in the corresponding Figure 39B) with $A = (1.6 \pm 0.15) \times 10^{-20} V^{-2} m^2$ In this figure the applied electric field E has been plotted in terms of V/N, N being the number of deposited monolayers. Obviously, the curves for $\Delta C/C$ versus V are not

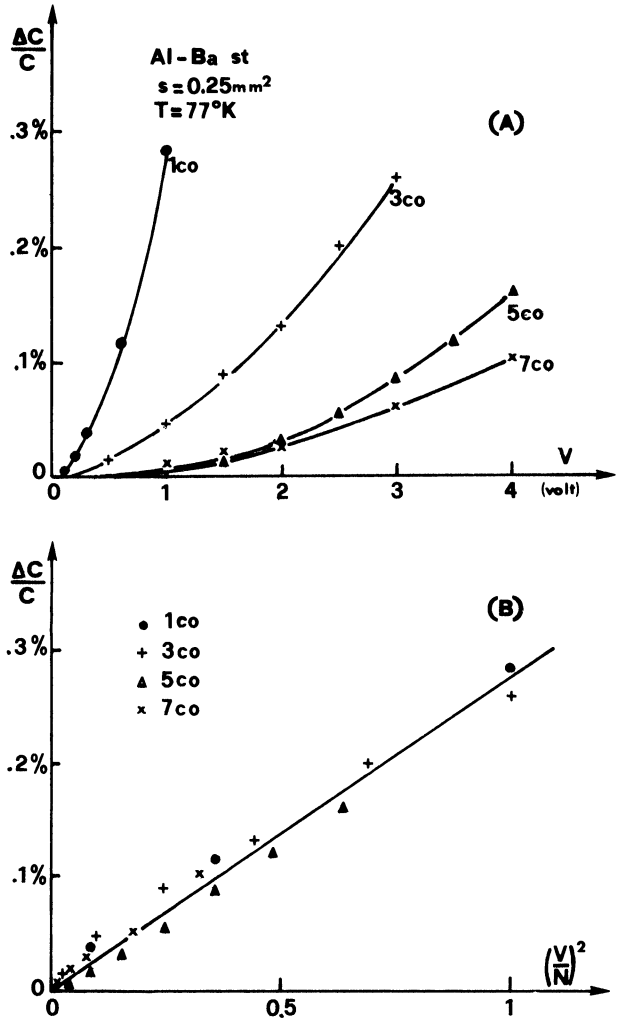

FIGURE 39 (A) Change of capacitance ΔC/C vs. applied voltage V for different number of Ba-stearate monolayers at temperature 77°K and area of the device = 0.25 mm² (B) Corresponding plot of ΔC/C vs. square of applied electric field (~ V^2/N^2). [After Leger *et al*[55].]

linear and this has been taken to be the evidence for an internal field inside the organic layers. These curves, which have a minimum for $V = 0 \pm 100$ mV, have been regarded as setting an upper limit for an internal field. The assumption that the linear dependence of capacitance on E^2 is due to the compression associated with the electrostatic pressure on the capacitance plates, leads to a compressibility coefficient of the stearate molecules which would be one order of magnitude larger than for bulk paraffins. Although such a value could be plausible, other phenomena, e.g. electrostriction action on the dielec-

tric constant of the insulator, should possibly be taken into account.

In the opinion of the author, it is hard to draw any conclusions from these preliminary measurements. The physical mechanism suggested by these workers does not appear to be conceivable until further measurements can be made. However, the presence of an internal field inside the monolayers reported by these workers has been verified further in the ionic transport studies of these structures, and some similar indications also come from the work of Tanguy.[152] As has been suggested by Leger *et al.*[55] themselves, the best course would be to repeat similar measurements on various organic substances, and to find out whether the order of magnitude of the compressibility coefficients of organic molecules is plausible.

9 FUTURE TRENDS AND PROPOSED APPLICATIONS

In fact, much has already been said regarding the future trends of research on Langmuir films. Nevertheless, to sum up, a few more remarks will be made which are of concern in any type of electrical studies of these films. Essentially, one of the challenging problems is to solve the riddle of the structure of Langmuir films. It has been regarded for a long time that the films obtained by B–L technique form "two-dimensional" crystals, whereas some recent investigations completely rule out this possibility, and indicate some structural changes inside the organic layers. Renewed structure studies are particularly important because all the electrical properties, by and large, are "structure sensitive". Another equally important aspect is to concentrate on many other organic substances, e.g. proteins, chlorophylls, dyes, esters, etc., which are eligible for monolayer formation and subsequent deposition by using the B–L technique. It is rather surprising that even in the recent investigations, the workers have not paid much attention to organic films other than those of fatty acids or their salts. Presumably, only French workers have made a breakthrough in this respect by studying orthophenanthroline molecules which were deposited by B–L technique. It is interesting to point out specifically the organic compound "cholesterol" ($C_{27}H_{45}OH$) which has been studied by some Russian workers[164] for "forming" and subsequent phenomena. In their studies, the monolayers or bilayers of cholesterol were obtained by a different technique, involving adsorption of polar molecules on a molecularly smooth surface of liquid mercury. However, these molecules in principle must also be obtainable by B–L technique, and efforts in this respect would be highly desirable. It has been reported by the Russian workers[164] (and references therein) that electrical studies on structured films of surface active organic molecules are of special significance to give information on the nature of phenomena occurring in biological membranes.

It has been noticed by several workers that Langmuir films deposited on gold base electrodes are shorting in nature, and that electrical measurements are not possible on such structures. On the other hand, with aluminium base electrodes, the oxide layer formation does complicate the situation in the interpretation of electrical data. There are some controversies in the existing literature about the influence of the oxide layer on the electrical properties of Langmuir films. For instance, some workers have taken into account the oxide layer, whereas others have neglected it, because of its low resistance as compared to that of the organic films. There are also few instances in which the electrical data could be interpreted in terms of the presence of an oxide layer in the device. The reason for obtaining shorting devices with gold base electrodes has been the poor adherence of molecules, and hence increasing porosity in the organic films. Despite the fact that some alternative metals have to be tried for the base electrodes to avoid oxide layer formation, the author proposes to take advantage of the recently developed thermal evaporation technique to obtain organic films on gold base electrodes. Comparison of studies performed on Langmuir films, and on evaporated organic films of the same substances on Al and Au electrodes respectively, may prove useful to separate out the influence of the oxide layer. The presence of water molecules adsorbed during monolayer transfer in the B–L technique can also be avoided if the renewed studies are performed on evaporated organic films. Fortunately, Baker[18] has pointed out that organic films can be obtained by thermal evaporation down to one monolayer in thickness and which possess more purity than the original evaporant. Scrupulous attention however, must be paid to the development of the thermal evaporation technique in future.

Despite the fact that Langmuir films have been reported to possess structural perfection, and could be obtained free from even a small fraction of holes and conducting impurities, it seems to be an optimistic view to consider these films ideally suitable for electrical studies and device applications. The problems which have hindered their use in the electronic

device application until now are the same as with many other film systems. For instance, problems with respect to stability of fatty acid films, which are soft, possess low melting points, and tend to collapse slowly with time. Although considerable efforts have already been expended to improve the deposition technique and to obtain stable films, in actual practice every new application requires a lot of painstaking work before Langmuir films with reproducible and stable electrical properties can be obtained. Nevertheless, some possible applications are discussed here to throw light on the status and role of Langmuir films, mainly in the electronics industry.

One of the most attractive applications of Langmuir films may be in the fabrication of "low loss capacitors" which find their use in active filters. For the choice of suitable material to fabricate a capacitor, one needs to consider many dielectric parameters, e.g. dielectric constant, dielectric strength dielectric loss, stability, temperature and voltage coefficients of capacitance, surface smoothness and insulation resistance. In the case of fatty acid films, several of these parameters are already known. For instance, the dielectric constant of stearate is 2.4, and films with capacitance densities 0.008 to 0.07 $\mu F/cm^2$ have been obtained. These films can also be deposited containing as many as 300 layers ($\simeq$ 7500 Å) and the capacitance has been found to vary only slightly with the frequency. The dielectric strength is a function of thickness, and it is of the order of 10^6 V cm^{-1}; dielectric losses $\simeq$0.02 to 0.006 have been reported. All these experimental values fulfil the optimum conditions to a greater extent for "low loss capacitors" as has been reported by Harrop and Campbell.[165] Fortunately, many organic polymers and other organic materials have already been used for this purpose.

Another possible application may be to develop tunnelling spacers between superconductors, as was attempted by Miles and McMahon[81] a long time ago. These workers failed to obtain useful tunnelling spacers simply because the device obtained showed highly non-linear characteristics. In fact, the deposition technique was not well developed in those days but now one may hopefully proceed in the light of recent advances. As for the controversy regarding conduction behaviour, whether it is dominated by tunnelling or by Schottky emission – the best test would be to study inelastic electron tunnelling between two metal films separated by organic insulating material. This technique of studying inelastic electron tunnelling was introduced by Jaklevic and Lambe[166,167] who distinguished it from the well-known tunnelling mechanism in which an electron goes through the barrier without energy loss. Inelastic tunnelling results in the energy transfer from electrons to the vibrational states of molecular species contained within the barrier. It has been pointed out that for such studies, the insulating film between two metal films must be about 50 Å thick and must support a field of 4×10^6 V cm^{-1}. This may, however, introduce some difficulties because the dielectric strength of a 50 Å thick organic film has been reported to be little lower,[109,121] but this is likely to be overcome in future investigations, as the dielectric strength measurements were made under atmospheric conditions rather than under vacuum.

Since Langmuir films have been shown to undergo "forming" and to exhibit voltage controlled negative resistance, some practical applications may be discussed which make use of such characteristics. The best use may be in the development of thin film resistive memory arrays based upon voltage controlled negative resistance in Langmuir films. Such a device was proposed by Nielson and Bashara,[168] and was described later by Simmons and Verderber[169] for SiO_X materials. Before making an attempt in this direction, it is necessary to study more carefully the memory switching of the diode and triode structures, and whether the information is stored in the form of permanent changes in the interior of the film. Similarly, one can also think of some "hot" electron devices. In these devices, the basic requirement is that of a metal-insulating film-metal structure in which the anode is sufficiently thin for hot electrons traversing the insulating film to be able to escape into the vacuum above. It has been shown by Gundlach and Kadlec[130,131] that the phenomenon of DNR may be attributed largely to the existence of filamentary conduction paths in these films. If the proposed filamentary conduction does exist in these devices, an attempt at this application would be worthwhile. As has already been pointed out, if electroluminescence is also exhibited in these films many more applications may be possible.

The application of Langmuir films in the form of metal-insulator-semiconductor devices is also possible, as Tanguy[152] successfully deposited these films on silicon surfaces. In fact MOS capacitors and transistors are already in the development stage, and therefore analogous MIS structures may also be considered for such devices. Presumably, MIS capacitors and transistors would be more successful than the corresponding MOS ones, because the organic films may be obtained largely free from defects, which, in the case of oxides, is rather difficult. The

use of organic films in the form of MIS structures also opens up another practical application for passivated dielectric films on silicon. Polymer films have already been shown to possess favourable properties for similar purposes[156]. The only difficulty may be due to the hysteresis phenomenon, but it must be surmountable by appropriate treatment of the silicon surface. It would also be advisable to explore the possibility of achieving controlled doping of an organic dielectric in the way that was attained with crystalline germanium and silicon. The fact that alternating monomolecular layers of different organic materials may be deposited one on top of the other, offers an exciting possibility for fabrication of some novel devices. One similar use of fatty acid monolayers has been in the form of distance keepers between dye molecules, while studying photographic sensitization mechanism.[88]

Having discussed some of the possible applications of Langmuir films, it is essential to point out once again that although these films possess many attractive features, unlike those of evaporated film systems, nevertheless one must not be too optimistic about all the suggestions made above. In addition to these electronic device applications, one of the most successful uses of Langmuir films has been in the fabrication of a fairly stable optical device called a "step gauge" or thickness gauge which is commercially available from General Electric Co., USA. Other optical applications of these films are worth mentioning, e.g. antireflection gratings and interference filters. From the purely scientific point of view, the resemblance of Langmuir films to biological membranes suggests that a careful study of these films would lead to the understanding of many biological or life processes. Some more industrial applications of these films are to achieve evaporation control[159] and to reduce friction,[170] etc.

Since only a handful of electrical data are available on Langmuir films, it would be unfair to make any committment regarding their practical applications. A few proposals made above in this respect are in a way speculative until these possibilities are explored further. Therefore, it seems to the author that the potential of Langmuir films still lies in the hands of experimentalists, and great developments in thin film technology will be achieved if efforts are continued. The application potential of these films is more likely to come from a systematic study of many diversified electrical phenomena. Of all the proposed applications, the development of capacitors is expected to come to the fore in the near future because of their use as electronic hardware components for thin film microcircuitry.

ACKNOWLEDGMENTS

The author wishes to express his sincere gratitude to Professor V. Celli for critical reading of the manuscript and for many helpful discussions. Thanks are due to Professors A. Many, C. A Neugebauer, N. H. March and G. Dearnley, who were at the International Centre for Theoretical Physics during the Winter College on Surface Science, for many useful suggestions to improve the text of the manuscript. The author is grateful to Dr. V. K. Srivastava, in particular, and to his other colleagues, who (while the author was in India) initially inspired him to write up the present manuscript. The preparation of the manuscript was initiated during the author's participation in the Winter College on Surface Sciences at the ICTP and completed during the following Workshop on Solid State Physics.

It is with great pleasure that the author expresses his thanks to the ICTP staff for all the co-operation and help without which work on this manuscript would have not progressed so smoothly. The author also wishes to thank Professor Abdus Salam, the International Atomic Energy Agency and UNESCO for hospitality at the International Centre for Theoretical Physics, Trieste. The author would be failing in his duties without acknowledging the permission granted by the respective authors and publishers of different research papers (and journals) for the reproduction of the figures and tables in the present review. The Swedish International Development Authority is gratefully acknowledged for making possible his associateship at the ICTP.

Last, but by no means the least, the author expresses his deep indebtedness and profound sense of gratitude to his parents, teachers and well-wishers for their invaluable encouragement time and again. The author finally dedicates this piece of work to an invisible but living force which, in fact, made him work to complete the survey.

NOTE ADDED IN PROOF†

Some measurements similar to those of Nathoo and Jonscher[91,96] have been carried out by Sugi *et al.*[171] using Cd-arachidate films. The a.c. admittance of Langmuir films has been measured by the two-terminal method. The frequency dependent characteristics of both the real and imaginary components of admittance, i.e. conductance and susceptance exhibited a linearity in the frequency region 100 Hz to 20 kHz. This almost linear law has been considered to be one of the common features of hopping conduction processes. However, a striking difference has been found in the order of magnitude of conductivity at 100 Hz with respect to the earlier work[91,96]. This difference has been ascribed to the experimental factors involved in the preparations of Langmuir films. In addition, thickness-dependent

†Thanks are due to Prof. H. Kuhn and Dr. E. P. Honig for mentioning to me these important works done in their respective places which had escaped my attention before.

conductance has been found to exhibit an anomalous behaviour, i.e. it is practically constant for 1 and 3 layers and then decreases monotonically with the number of layers approaching to a constant value. It is regarded to be the first and direct evidence for contact effect and explained it tentatively by assuming a highly conductive region near each electrode in accordance with the suggestion given by Jonscher (cf. ref. 171). The susceptance with respect to thickness, however, does not show such anomalous behaviour.

Subsequently the same workers[172] studied dye-sensitized Langmuir films, developing two types of one dimensional structures with a different but periodic arrangement of dye and arachidate molecules. The photo-induced increment of a.c. conductance (ΔG) studied in this work revealed the finer details of $\Delta G-\omega(\omega$,frequency) characteristics. Each of the characteristics exhibited a hump or two at a certain frequency range whose location has also been determined. The humps at frequencies are found to decrease exponentially with increasing thickness of the constituent monolayers. The estimated value of N_t (density of the interface) has been found to differ in the two types of structures which is explained in terms of the higher concentration of molecular chains of Cd-arachidate in one of these two. Regarding the nature of humps, nothing seems to have been committed, rather, these are assumed to correspond to the characteristic relaxation times of quantum-mechanical hopping governed by the one-dimensional super-structure associated with the film.

In a very recent work of Sugi and co-workers[173], the high field photo-conduction is studied systematically in Langmuir films which were periodically arranged with dye sensitizers. The capacitor type junctions were obtained by the molecular assembling technique[174] (essentially a modified, L–B technique) using Cd-arachidate and surface active merocyanine dye. The photo-conduction is found to be the bulk effect due to the chromophores for thickness higher than 400 Å. Further, each of the temperature dependent characteristics has been observed to undergo a change in its slope at 290°K whose value depends upon bias polarity and magnitude both above and below this transition region. The high temperature mode is then associated with the activation energy. The voltage dependence of photocurrent showed a non-ohmic behaviour for both the lower and higher temperature modes. They[173] have thus interpreted that higher temperature mode occurs due to the thermionic process in which electrons are released from the chromophores of the dye sensitizer into the conduction band. The lower temperature mode is characterised to be a consequence of quantum-mechanical hopping process. In the opinion of the author, the work of Sugi *et al.* is an important and thorough contribution to enhance our understanding about the underlying conduction mechanism in Langmuir films. Some details about the basic electronic properties of these systems are also given, unlike in the previous works which, hopefully, should activate our interest in theoretical aspects of Langmuir films.

For experimental details to obtain periodic mixed monolayer assemblies of fatty acid salts and dye molecules, their physical properties and the optical behaviour of such systems, the reference is made to a comprehensive review of Kuhn et al.[174] Some of the electrical properties are also described in this review. It would be worthwhile to mention a few more references[175–178], which are concerned mainly to the deposition technique of Langmuir films (sophisticated one, avoiding the use of silk thread and piston oil as described in the present paper), some of the physical properties and thickness determination by using ellipsometric method. It seems that ellipsometry is a better method than multiple beam interferometry. A final remark should be made that Agne Pockels[179], in fact, had invented the basic technique of handling monolayers in 1891 which was modified and given a practical shape later by Blodgett and Langmuir[5,6].

REFERENCES (Contd. from Part 1)

99. Fock, *Arch. Elektrotech.*, **19**, 71 (1927).
100. N. Klein and H. Gafni, *IEEE Trans. Electron Devices* **ED13**, 281 (1966).
101. N. Klein, *Thin Solid Films* 7, 149 (1971).
102. A. von Hippel, *Naturwiss enschaften* **14**, 79 (1935).
103. H. Fröhlich, *Proc. R. Soc.*, **160**, 230 (1937); **172**, 94 (1938).
104. F. Forlani and N. Minnaja, *Phys. Status Solidi* **4**, 311 (1964).
105. F. Forlani and N. Minnaja, *Nuovo Cimento*, **31**, 1246 (1964).
106. P. P. Budenstein and P. J. Hayes, *J. Appl. Phys.*, **38** 2837 (1967).
107. P. P. Budenstein, P. J. Hayes, J. L. Smith and W. B. Smith, *J. Vac. Sci. and Technol.*, **6**, 289 (1969).
108. J. L. Smith and P. P. Budenstein, *J. Appl. Phys.*, **40**, 3491 (1969).
109. V. K. Agarwal and V. K. Srivastava, *Thin Solid Films*, **8**, 377 (1971).
110. V. K. Agarwal and V. K. Srivastava, *Thin Solid Films*, **13**, S23 (1972).
111. F. Forlani and N. Minnaga, *J. Vac. Sci. and Technol*, **6**, 518 (1969).
112. F. Seitz *Phys. Rev.*, **76**, 1378 (1949).

113. H. Fröhlich and B. V. Paranjape, *Proc. Phys. Soc. (London)*, **B69**, 866 (1956).
114. J. J. O'Dwyer, *J. Phys and Chem. Solids*, **28**, 1137 (1967).
115. J. J. O'Dwyer, *J. Appl. Phys.*, **40**, 3887 (1969).
116. N. Klein, *Adv. Phys.*, **21**, 605 (1972).
117. D. B. Watson, W. Hayes, K. C. Kao and J. H. Calderwood, *IEEE Trans. Electr. Insul.*, **5**, 58 (1970).
118. W. Shockley, *Solid-State Electron*, **2**, 35 (1961).
119. J. J. O'Dwyer, *The Theory of Dielectric Breakdown in Solids* (Oxford University Press, London, 1964).
120. P. A. Thiessen, D. Beischer and H. Gillhausen, *Frhr. v. Naturwiss enschaften*, **28**, 265 (1940).
121. V. K. Agarwal and V. K. Srivastava, *Solid State Commun.*, **12**, 829 (1973).
122. V. K. Agarwal and V. K. Srivastava, *Electrocomponent Sci. and Tech.*, **1**, (1974).
123. V. K. Agarwal and V. K. Srivastava, *J. Appl. Phys.*, **44**, 2900 (1973).
124. V. K. Agarwal and V. K. Srivastava, *Thin Solid Films*, **14**, 367 (1972).
125. V. K. Agarwal and V. K. Srivastava, *Solid State Commun.*, **11**, 1461 (1972).
126. V. K. Agarwal, *Thin Solid Films*, **22** S3, (1974).
127. V. K. Agarwal *Thin Solid Films*, **22** S9, (1974).
128. N. Klein, *Adv. Electron and Electron. Phys.*, **26**, 309 (1969).
129. N. Klein and N. Levanon, *J. Appl. Phys.*, **38**, 3721 (1967).
130. K. H. Gundlach and J. Kadlec, *Phys. Status Solidi (a)*, **10**, 371 (1972).
131. K. H. Gundlach and J. Kadlec, *Thin Solid Films*, **13**, 225 (1972).
132. G. Dearnley, A. M. Stonehame and D. V. Morgan, *Rep. Prog. Phys.*, **33**, 1129 (1970).
133. R. R. Verderber, J. G. Simmons and B. Eales, *Philos. Mag.*, **16**, 1049 (1967).
134. R. R. Verderber and J. G. Simmons, *Radio & Electron. Eng.*, **33**, 347 (1967).
135. T. W. Hickmott, *J. Appl. Phys.*, **33**, 2669 (1962).
136. T. W. Hickmott, *J. Appl. Phys.*, **35**, 2118 and 2679 (1964).
137. C. Barriac F. Giraud-Hiraud, P. Pinnard and F. Davoine, *C. R. Acad. Sci.*, **262**, 900 (1966).
138. C. Barriac, P. Pinnard and F. Davoine, *C.R. Acad. Sci.*, **266**, 423 (1968).
139. C. Barriac, P. Pinnard and F. Davoine, *Phys. Status Solidi*, **34**, 621 (1969).
140. G. Dearnley *Phys. Lett.*, **25A**, 760 (1967).
141. J. F. Gibbons and W. E. Beadle, *Solid-State Electron.*, **7**, 785 (1964).
142. R. R. Sutherland, *J. Phys. D.*, **4**, 468 (1971).
143. J. G. Simmons and R. R. Verderber, *Proc. R. Soc. A*, **301**, 77 (1967).
144. J. Bernard, R. Hang, Y. Mentalecheta and Y. Tregouet, *Phys. Status Solidi*, **6**, K127 (1971).
145. J. Curie, *C.R. Acad. Sci.*, **130**, 930 (1886).
146. E. Warburg and F. Togetmeier, *Ann. Phys. (Germany)*, **35**, 455 (1888).
147. C. Bucci and R. Fieschi, *Phys. Rev. Lett.*, **12**, 16 (1963).
148. A. Joffe, *The Physics of Crystals* (McGraw-Hill, New York, 1928).
149. R. W. Dreyfas, *Phys. Rev.*, **121**, 1675 (1961).
150. Y. Haven, *J. Chem. Phys.*, **21**, 171 (1953).
151. G. D. Watkins, *Phys. Rev.*, **113**, 91 (1959).
152. J. Tanguy *Thin Solid Films*, **13**, 33 (1972).
153. E. H. Snow, A. S. Grove, B. E. Deal and G. T. Sah, *J. Appl. Phys.*, **36**, 1664 (1965).
154. T. L. Chu J. R. Szedon and C. H. Lee, *Solid-State Electron*, **10**, 897 (1967).
155. S. R. Hofstein, *Solid-State Electron.*, **10**, 657 (1967).
156. A. Bui H. Carchano and D. Sanchez, *Thin Solid Films*, **13**, 207 (1972).
157. A. Goetzberger, V. Heine and E. H. Nicollian, *Appl. Phys. Lett.*, **12**, 95 (1968).
158. W. E. Dahlke and S. M. Sze, *Solid-State Electron.*, **10**, 865 (1967).
159. V. K. LaMer, *Retardation of Evaporation by Monolayers* (Academic Press, New York, 1962).
160. C. Bucci, R. Fieschi and G. Duidi, *Phys. Rev.*, **148**, 816 (1966).
161. C. A. Bucci and S. C. Riva, *J. Phys. & Chem. Solids*, **26**, 363 (1965).
162. A. Servini and A. K. Jonscher, *Thin Solid Films*, **3**, 341 (1969).
163. A. K. Jonscher, *Thin Solid Films*, **1**, 213 (1967).
164. A. S. Babaev, V. V. Kuznetsova and V. I. Stafeev, *Sov. Phys.–Semicond.*, **7**, 692 (1973).
165. P. J. Harrop and D. S. Campbell, *Thin Solid Films*, **2**, 273 (1968).
166. R. C. Jaklevic and J. Lambe, *Phys. Rev. Lett.*, **17**, 1139 (1966).
167. J. Lambe and R. C. Jaklevic, *Phys. Rev.*, **165**, 821 (1968).
168. P. H. Nielsen and N. M. Bashara, *IEEE Trans. Electron Devices*, **ED–11**, 243 (1964).
169. J. G. Simmons and R. R. Verderber, *Radio & Electron. Eng*, **35**, 265 (1968).
170. D. Tabor, *Surface Colloid Science* (John Wiley, New York, 1972), **Vol. 7**.
171. M. Sugi, K. Nembach, D. Möbius and H. Kuhn, *Solid State Commn.*, **13**, 603 (1973).
172. M. Sugi, K. Nembach, D. Möbius and H. Kuhn, *Solid State Comm.*, **15**, 1867 (1974).
173. M. Sugi K. Nembach and D. Möbius, *Thin Solid Films*, (To appear).
174. H. Kuhn, D. Möbius and H. Bücher, *Techniques of Chemistry* (eds. A. Weissberger and B. W. Rossiter), (Wiley, New York 1972), Vol. I, part III B, pp. 577–702.
175. D. den Engelson, *J. Opt. Soc. Am.*, **61**, 1460 (1971).
176. E. P. Honig, *J. Colloid Interf. Sci.*, **43**, 66 (1973).
177. D. den Engelson *J. Colloid Interf. Sci.*, **45**, 1 (1973).
178. E. P. Honig, J. H. Th. Hengst and D. den Engelson, *J. Colloid Interf. Sci.*, **45**, 92 (1973).
179. A. Pockels, *Nature*, **43**, 437 (1891).

REFERENCES CITED IN PART I

1. V. K. Agarwal, *Thin Solid Films*, **24**, 55 (1974).
5. K. B. Blodgett, *J. Am. Chem. Soc.*, **57**, 1007 (1935).
6. K. B. Blodgett and I. Langmuir, *Phys. Rev.*, **51**, 964 (1937).
18. M. A. Baker, *Thin Solid Films*, 8, R13 (1971).
29. L. Holt, *Nature*, **214**, 1105 (1967).
38. G. Marc and J. Messier, *J. Appl. Phys.*, **45**, 2832 (1974).
43. H. H. Race and S. I. Reynolds, *J. Am. Chem. Soc.*, **61**, 1425 (1939).

45. A. Barraud, J. Messier, A. Rosillo and J. Tanguy, *Colloque AVISEM, Versailles,* (Sept. 1971).
46. E. F. Porter and J. Wyman, Jr., *J. Am. Chem. Soc.,* **60**, 1083 (1938).
53. K. H. Drexhage and H. Kuhn, *Basic Problems in Thin Film Physics,* (Göttingen, Vandenhoeck and Ruprecht, 1966) 339.
55. A. Leger, J. Klein, M. Belin and D. Defourneau, *Thin Solid Films,* 8, R51 (1971).
63. J. Tanguy and P. Hesto, *Thin Solid Films,* **21**, 129 (1974).
69. J. J. O'Dwyer, *The Theory of Electrical Conduction and Breakdown in Solid Dielectrics,* (Clarendon Press, Oxford, 1973).
70. R. H, Fowler and L. Nordheim, *Proc. R. Soc. A,* **119**, 173 (1928).
81. J. L. Miles and H. O. McMahon, *J. Appl. Phys.,* **32**, 1176 (1961).
88. B. Mann, H. Kuhn and L.v. Szentpaly, *Chem. Phys. Lett.,* 8, 82 (1971).
90. V. K. Srivastava, *Phys. Rev. Lett.,* **30**, 1046 (1973).
91. M. H. Nathoo and A. K. Jonscher, *J. Phys. C,* 4, L301 (1971).
96. A. K. Jonscher and M. H. Nathoo, *Thin Solid Films,* **12**, S15 (1972).